NASA Contractor Report 172160

Technology Evaluation of Man-Rated Acceleration Test Equipment for Vestibular Research

I.Taback,R.L.Kenimer,and A.J.Butterfield

The Bionetics Corporation
Hampton,VA.23666

Contract NAS1-16978
September 1983

National Aeronautics and
Space Administration

Langley Research Center
Hampton, Virginia 23665

TABLE OF CONTENTS

TABLES

FIGURES

FIGURES (CONT'D) Page

Technology Evaluation of Man-Rated Acceleration Test Equipment For Vestibular Research

I. Taback, R. L. Kenimer,
and A. J. Butterfield

The Bionetics Corporation
Hampton, VA 23666

SUMMARY

Vestibular experiments which involve linear cyclic motions require test equipment which does not generate any cyclic spurious acceleration pulses or noises which can be sensed by the test subject as "cues" to the applied motion. Acceleration cues coincident with the change in the direction-of-motion are a principal concern. This study establishes some design limits for acceleration cues, identifies the noise sources and levels in some of the present items, and describes some technical approaches to noise free systems which could be used in both ground and shuttle testing.

The establishment of the design limits for acceleration cues was based upon published experimental measurements for human thresholds of perception to linear cyclic motion. The design limit shows 0.01g (0 to peak) at 0.04 Hz and drops to 0.0003g (0 to peak) at 3 Hz. The limit is constant to 10 Hz where it begins to increase and reaches 0.001g (0 to peak) at 100 Hz. The published measurements indicate that humans show a maximum sensitivity to motion or acceleration effects over the range of 3 Hz to 10 Hz.

The identification of noise sources and levels were based upon measurements from existing vestibular research sleds. Horizontal systems based upon linear ball bearings and tensioned, wrapped-cable drives encounter non-linear friction effects and hysteresis effects which will result in motion-reversal cues up to 0.03g (0 to peak). These values exceed the thresholds for human perception. The motion reversal transients have been eliminated in a hydraulically-driven vertical system; however, such massive units are not compatible with shuttle flights.

The technical approaches to a low noise system involve the use of air bearings for the carriage supports and either linear induction motors or metal belts for the drive. Moving coil linear induction motors operating at the lowest practical frequency (i.e. 10 Hz) offer the most attractive option. Metal belts running on air bearing pulleys present the other achievable option.

The conduct of the study identified a number of testing techniques which could be employed for preliminary type investigations, and some of these approaches are compatible with testing in the mid-deck of the shuttle. These are discussed in the appendix in terms of pendulums, linear motion devices and adaptations of commercial air bearing tables.

1.0 INTRODUCTION

The technical evaluations of man-rated test equipment and the related technology stemmed from a potential NASA need for a flight sled which could provide low frequency oscillatory motions with all extraneous acceleration excitations (spurious noises) held below the thresholds for human perceptions. The operating concern focused upon the elimination of acceleration noises in the system which could cue a test subject such that the measurements obtained reflected more than just the desired otolith/

vestibular response to the accelerations applied or velocities attained. The elimination of spurious excitation cues coincident with zero velocity (change-of-direction for motion), appeared as a requirement for the operation of the sled during oscillatory tests. Ground test operations with sleds have shown that spurious excitations do occur coincident with change-of-direction and these noises have been associated with such sources as friction in bearings and hysteresis in drive cables.

The evaluation began with a review of published measurement data for thresholds of human perception to linear oscillatory motions. These measurements served to define the limits for spurious noises and acceleration cues. A series of measurements performed on existing sleds identified the sources and defined the existing excitation levels for spurious noises and acceleration cues. The evaluations of technology identified the improvements required or approaches to designs necessary to keep spurious noises and any acceleration cues below the levels of perception. The sections which follow present the results and findings from each of these areas in the order described. In the course of the technical evaluations, concepts for test equipment arose which could support preliminary or screening type of experimentation. These concepts were based upon pendulums, flexures and industrial air bearing tables. They could offer an investigator a means for early identification of an effect such that he could either define a more comprehensive approach to the research or avoid an unproductive course. The Appendix presents a descriptive compilation and discussion of these concepts.

The authors wish to acknowledge the dedicated cooperation and support they received during the conduct of this study: The NASA/Ames Research Center provided the instrumentation, data analysis equipment, and an operating team of Mr. Robert Mah (ARC) and Mr. Howard Mensch of the Syscon

Corporation. Their efforts produced the definitive measurements and data for existing sleds and for air bearings which were necessary for the effective conduct of the evaluation. The cooperation and support extended by Dr. Lawrence Young and his associates in the Man Vehicle Laboratory at the Massachusetts Institute of Technology provided the opportunity for obtaining the detailed measurement needed to identify and define the particular sources of acceleration cues. The cooperation and support extended by Dr. William H. Bush and his associates in the Life Sciences Laboratory at the NASA/Lyndon B. Johnson Space Center provided the opportunity to obtain the baseline dynamic data pertinent to evaluating the operation of a man-rated research sled.

2.0 SYMBOLS

A	Cross-sectional area of a metal belt, m^2, A = wt
a	Acceleration m/sec^2
E	Modulus of elasticity for material, Pa
F	Force, N
f	Coeficient of friction
g	Acceleration due to earth gravity, 9.8 m/sec^2 (n) g maximum vibrational acceleration in term of earth gravity units
grms	Vibration acceleration, root mean square (0.707)(g max)
r	Radius of a drive drum
S	Stress, Pa
T	Tension Force, N
t	Thickness of a belt, m
w	Width of a belt, m
X	Angle defining the wrap of a belt around a driving drum, radians
Δ	Small angular increment radians
ϵ	Local strain, m/m
ρ	Radius of curvature, m
T	Strain energy in a unit length of belt $\frac{Nm}{m}$

SUBSCRIPTS

max	Maximum value
min	minimum value
u	useful

3.0 THRESHOLD OF PERCEPTION MEASUREMENTS AND DEFINITION OF LIMITS

The requirement for an acceleration test facility in which the test subject would not feel any acceleration cues implied a knowledge of the thresholds for human perception across the entire spectrum of frequencies which could be encountered in a testing situation. Therefore, in a corrolary assumption, a survey of published measurement data would provide the basis for defining a practical limit for use as a design criteria. Accordingly, the survey of measurement data contained three elements, the extraction of usable data, an assessment of pertinence, and the construction of a practical limit.

3.1 Literature Survey, Data Sources

A substantial body of published research data addresses human and non-human responses to acceleration environments. Within that body a recent compilation by Gundry (ref. 1) summarizes the measurements from research studies involving thresholds-of-perception for periodic linear motion. This compilation plus some subsequent measurements represented the source data to construct a design limit characteristic for spurious noise excitations or acceleration cues in man-rated vestibular research equipment. In reviewing the data, some of the original papers referenced by Gundry were obtained (and translated) as an aid toward understanding the details of the experimental techniques employed. In surveying the literature on threshold measurements, the largest portion appeared to address the sensitivities of air crews to vibrations. Other bases for measurement included the general study of human body responses to vibration (von Bekesy, ref. 2) and the definition of limits for the movement of buildings (Chen and Robertson, ref. 3). The compilation by Gundry was part of a general dissertation on human responses; the data presented included steady state linear motion and latency responses, as well

as responses to cyclic motion. For cyclic motions, the discussion addressed the effects of visual cues on thresholds, effects of partial accelerations (feet on an unmoving floor, etc.) and estimated the mode or portion of the body which provided the principal sensory response to vibration in terms of the applied frequency. While responses to cyclic motion were the common feature for the data presented, the defining of a design limit from the compilation of measurements had to make a selection of measurements considered pertinent to such a determination. The criteria for selection became:

1. The measurements should be limited to just whole body responses. Thresholds that involved visual cueing or acceleration of only a portion of the body were excluded.
2. The measurements should represent a group of individuals tested without any previous conditioning or opportunity to "learn" the system.
3. The measurements should involve test subjects in ordinary positions such as standing, sitting, prone, etc., and have the direction of the acceleration parallel to one of the axes defined for the body according to aircraft conventions.

These concepts are further described in Section 3.2 below; the data extracted from Gundry and subsequent measurements are listed in Table 3-1. The measurements corresponding to each "Data Point" listing appear in figure 3-1 which is an extraction from Gundry (ref. 1, figure 1). For sources taken directly from Gundry, the references also include his listing [e.g., Chaney (4)]. Sources which were individually analyzed or translated have separate references.

TABLE 3-1. SUMMARY OF THRESHOLD-OF-PERCEPTION DATA SOURCES

DATA POINT	SOURCE	TEST RIG	TEST SUBJECTS/ACCOMMODATIONS	ACCELERATION/ DIRECTIONS ON TEST SUBJECT
1	Chaney 1(4)	Vertical Axis Shaker	10 males, seated with lap belt restraint and footrests. Each subject makes 4 determinations at 4 frequencies (8 measurements for each frequency data point).	Z-Z
2	Chaney 1(5)	Vertical Axis Shaker	5 males, standing, feet attached to moving platform.	Z-Z
3 4	Chen and Robertson 3	Closed room on a platform with 2-axis horizontal motion	2 subjects at each frequency, standing.	3 X-X 4 Y-Y
5 6 7	Chen and Robertson 3	Closed room on a 25m pendulum	10 subjects sitting. 10 subjects sitting. 20 subjects standing.	5 X-X 6 Y-Y 7 X-X
8	Goril and Snyder 1(8)	Vertical Axis Shaker	6 males (air crew) seated in a cockpit simulation.	Z-Z
9	Gurney 1(12)	Vertical circular arc 3.26m radius	3 subjects sitting blindfolded (seesaw).	Z-Z
10	Landsberg 1(18)	3.6m Pendulum	Subjects lay face-down and face-up.	Z-Z
11 12	Richer and Meister 1(22)	Platform driven by eccentric mass vibrator	10 subjects in five positions; Standing, X-X, Z-Z; lay face-up X-X, Y-Y, Z-Z. (12 is X-X face up only.)	11, All 12, X-X
13	von Bekesy 2	2m Horizontal circular arc	2 subjects seated	Y-Y
14 15 16	Walsh 1(24)	1.55m Pendulum	4 to 7 subjects each test point. Lay face-up, face-down, on sides. 8 measurements for each subject.	14, X-X 15, Y-Y 16, Z-Z
17	Walsh 1(26)	Vertical circular arc	7 males, 4 measurements each, 8 times. Lay face-up.	X-X
18	Benson	Vertical hydraulic driven oscillator	6 males, 4 females in an aircraft ejection seat.	Z-Z
19	Bionetics at Miami U.4	4m Pendulum	2 males lay face-down, series of measurements at one frequency.	Y-Y

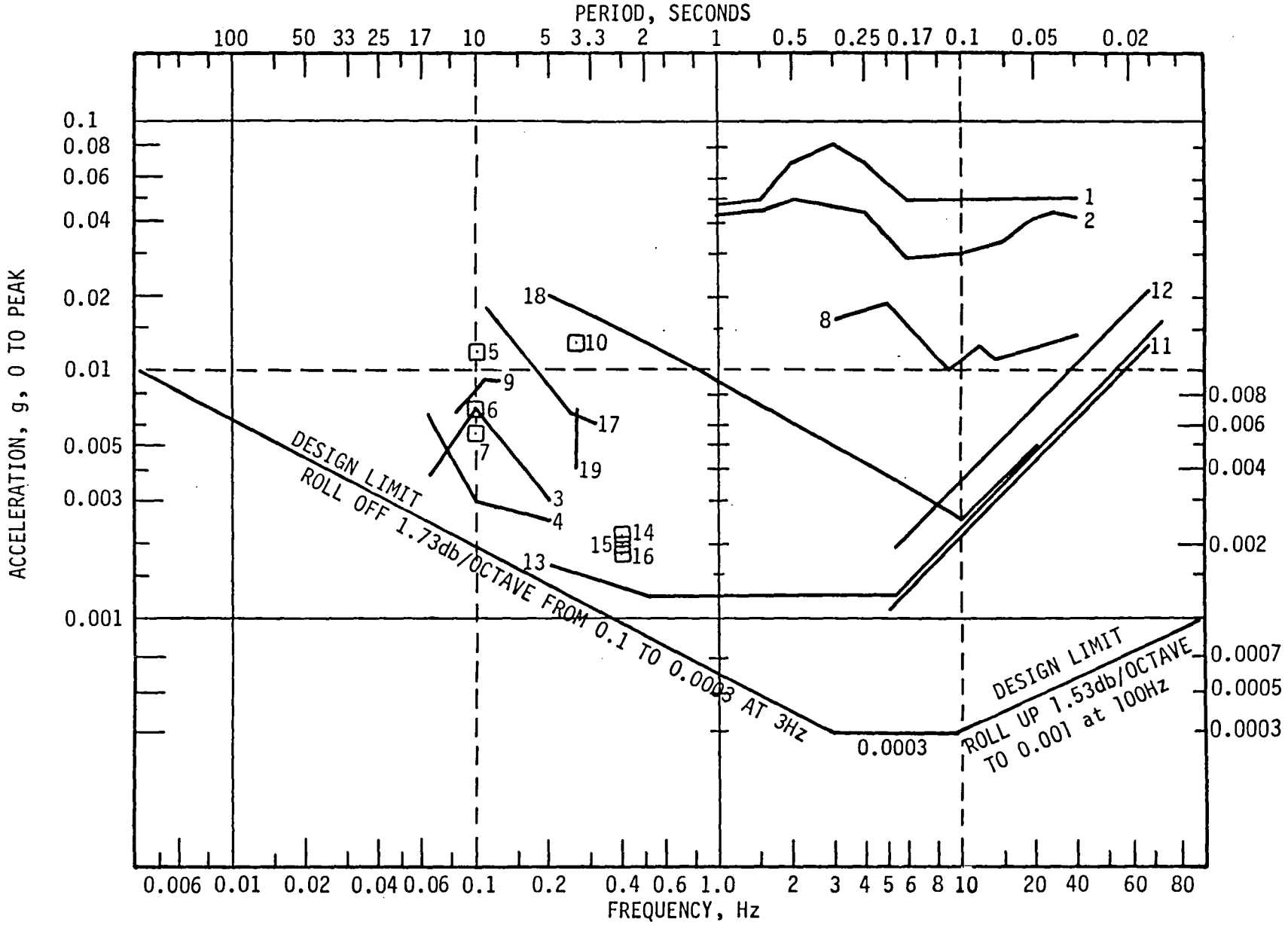

Figure 3-1. Threshold-of-Perception Measurements and a Design Limit For Spurious Accelerations

A review of the measurements data as presented in figure 3-1 shows a consistent pattern across the range of frequencies applied. The upper frequency limit of 100 Hz is somewhat arbitrary. Within the human system the mode for sensing oscillation begins to involve more than the vestibular elements as frequencies increase beyond about 1 Hz (ref. 1). At 100 Hz, sensing appears to have become almost entirely a skin (tactile) response and 100 Hz appears to be a practical upper limit for much of the test equipment utilized (hydraulic shakers and mechanical-arm links). At the lower frequencies, test equipment also effectively limits the cyclic forces which can be applied. For very low frequencies pendulum rigs require lengths beyond the capability of most buildings (e.g., Chen - 25 meters). Other low frequency oscillating systems are not available (testing at 0.01 Hz involves a movement through 50 meters to apply a sinusoid acceleration of 0.01g). Within such limitations, the data sources listed in Table 3-1, and their corresponding measurements shown in figure 3-1, are considered the best available for defining a spurious noise or acceleration cue design limit for threshold-of-perception sensitive test equipment.

3.2 Data Assessment, Validity

The assessments for validity of the data considered the frequency dependence of human responses to linear accelerations, the effects of the earth imposed gravity field and the need for data which appeared to have statistical consistency relative to the method-of-test and the population measured.

3.2.1 Human Responses to Frequency of Accelerations

Research reported in the literature has proposed analytical models to describe human responses as a function of the frequency for applied accelerations. The principal area which appears unresolved involves the conditions associated with the change from linear-sustained to linear-

sinusoidal (frequency range 0 to 0.1 Hz). The models presented however are all single-valued in terms of responses and frequencies; no model postulates a discontinuity. The construction of a design limit therefore is governed by that concept. The limit must be a continuous and single valued function of frequency. Some of the measurements indicate a localized change in threshold-of-perception (figure 3-1 Chaney 1,2, Walsh 17) however none of the local effects involve as much as an order of magnitude (a factor of 2 covers most). These local effects still remain within the context of single-valued and continuous with frequency.

From these measurements it appears that if an individual is subjected to a complex wave which contains all frequencies at the same relative level, then he will sense that complex wave at the frequency for which he has the lowest threshold. In corrolary, if an individual is subjected to a complex wave that contains discrete frequencies at different levels, he will sense that wave at the specific discrete frequency which first exceeds his threshold for that specific frequency. These response considerations suggest that a design limit characteristic can be defined in a manner which follows the overall response pattern for humans but maintains a realistic margin below measured thresholds.

3.2.2 Earth Gravity Field

The entire body of thresholds data may be considered in terms of the vector addition of a small, cyclicly varying force plus the gravity field of the earth. The variable vector associated with the applied force remains less than 10 percent of that imposed by gravity. The measurement data considered for definition of limits includes four cases for such vector addition which summarize in order of decreasing total vector sum as:

a) Vertical oscillations; The applied accelerations either add or subtract directly from the gravity force. The maximum vector difference is

two times the applied peak acceleration (Data Points 1, 2, 8, 9, 11, 12, 17, and 18).

b) Circular Arcs from the Vertical (Gravity Driven Pendulums): For these measurements, the peak applied accelerations are considered perpendicular to the gravity force; however, at the bottom of the swing, a centrifugal (velocity) acceleration adds to the gravity vector (Data Points 5, 6, 7, 10, 14, 15, 16, and 19).

c) Circular Arcs in a Horizontal Plane (Driven Horizontal Arm Suspended by Flexures): In this mode, both the applied and centrifugal accelerations are in the horizontal plane and perpendicular to the gravity vector (Data Point 13).

d) Horizontal Linear Motions: In this mode the applied acceleration is always perpendicular to the gravity field with no secondary effects (Data Points 3 and 4).

The measurements from each type of testing overlap and the differences between individual subjects during a measurement sequence appears as great as any difference due to the direction of the applied excitation. Consequently for human subjects, a threshold-of-perception limit can be based upon any of the techniques described and apply to any direction of excitation.

3.2.3 Test Subjects and Population

It appears reasonable to postulate that each person has an individual threshold-of-perception characteristic, and the population as a whole would show some type of statistical distribution. The definition of a design limit needs to identify the lower edge of that statistical distribution. Therefore, useable data must represent a population of test subjects. In a further consideration, the literature surveyed included measurements which addressed changes in thresholds after some pre-condi-

tioning or acceleration exposure (ref. 4); none of the measurements showed thresholds of perception lower than those measured from "unconditioned" test subjects. Consequently, data from unconditioned test subjects were selected for defining a desgin limit.

The survey of literature also included studies which address vestibular responses along the principal axes of vestibular sensitivity and these directions do not coincide with the types of motion associated with most flight-related activities. The usual mode for sensing of accelerations or motions by human subjects appears to be a combined or shared response within the elements of the vestibular systems. The positions which humans could assume in conducting flight operations or similar on-board activities became the basis for selection of measurement data and relative to the head they followed the established convention (ref. 5).

Axis X-X Forward - backward, in the direction of the nose and eyes.

Axis Y-Y Side to side - in the direction of the ears.

Axis Z-Z Up and down - in the direction of the top of the head.

In these motions, the only requirement on the position of the body was a straight spine. Sitting, standing or laying down were considered acceptable. The summary of measurements does not show any significant differences which can be associated with a preferential axis or position of the body.

3.2.4 Population Statistics

The surveying of measurement data recognized that thresholds-of-perception determination could often be a portion of a larger research study. Such measurements are inherently usable regardless of source. The measurements considered most useful appear where a good population of subjects has been tested and the measurements repeat. Such measurements can be used to establish limits for particular frequencies, the balance of the

data then serves to define the trend for the threshold limit characteristic. In reviewing the source data, the work of Chen and Robertson (Data Points 5, 6, and 7) appears to offer measurement repeatability with statistical consistency. In the long radius pendulum measurements at 0.1 Hz, the number of subjects was statistically significant. The mode of testing required the subjects to actively focus their attention on an object (art); and, they were isolated from any other excitation except motion (by means of a closed room). These conditions resulted in measurements of consistent high quality. The work of Chen is considered the most definitive for linear motion at 0.1 Hz. The measurements by Von Bekesy (Data Point 13) carry a similar value of definition accuracy. The use of the driven horizontal circular-arc pendulum allowed precise control of frequency and showed good repetition between subjects. Measurements by Von Bekesy over the range 0.8 to 8 Hz are considered to be the definitive data for that range. The correlation offered by Richer and Meiser (Data Points 11, 12) for the range 1 Hz to 40 Hz confirm the observations.

3.3 Definition of a Spurious Excitation Design Limit

The limit for spurious acceleration noise applicable to the design of man-rated vestibular test equipment appears as the heavy line so-identified in figure 3-1. The generation of the characteristic utilized the following premises or assumptions:

1. Frequency Range 3 Hz to 10 Hz. Humans appear to have their most sensitive thresholds-of-perception over this range of excitation frequencies. The design limit level has been placed at a value of 0.0003g, 0-to-peak (0.00021 grms) and provides a factor of 3 margin below the lowest measured thresholds over that frequency range.

2. Frequency Range 10 Hz to 100 Hz. The slope (roll up) at 1.53 db/octave from 10 Hz to 100 Hz was configured to provide an order-of-magnitude margin for excitations above 25 Hz. The frequency range 10 Hz to 100 Hz was considered to include the majority of the potential acceleration cues or spurious noises; consequently, the margin has been increased.
3. Frequency Range 0.004 Hz to 3 Hz. The slope (roll off) at 1.73 db/octave has been based upon a factor of 3 margin below the lowest measurements by Chen and Robertson (Data Point 6), a factor of two margin below the measurements by Walsh (Data Point 16) and to remain below any measurements by Von Bekesy (Data Point 13). The margin is considered conservative; for frequencies below 1 Hz, sources of equipment-related acceleration cues are not obvious.

4.0 EVALUATION OF EXISTING ACCELERATION SLEDS

The evaluation of existing man-rated acceleration test sleds for acceleration noises and their corresponding levels of dynamic response proceeded as a companion effort to the review of published literature. A number of existing sleds were candidates for evaluation however only four received attention. The candidates and the types of evaluations performed are summarized in Table 4-1. The results from the evaluations are described in the order presented in the table; the first series of measurements were obtained from the sled at JSC which was not a completed unit at the time. These results were considered as pathfinders to permit a selective focusing for the evaluations at MIT which provided the more definitive data.

4.1 Measurements from the Acceleration Test Sled at MIT

The measurements obtained from the MIT Sled concentrated upon three principal effects or considerations pertinent to the control of motion. Specifically, the measurements sought data to define:

1. The effects produced by the bearings during rolling friction, during starting (or stopping) friction and measurements of the discontinuity during reversals of motion.
2. The effects produced by the tensioned cable drive system in terms of both the frequency and magnitude of induced vibration plus any effects caused by a change in direction-of-motion.
3. Sources and levels of other noises or disturbances such as off-axis responses and responses transmitted from the building itself.

TABLE 4-1. SUMMARY OF MAN-RATED ACCELERATION TEST SLIDES CONSIDERED FOR EVALUATIONS

	SLED LOCATION-DESCRIPTIONS	ACTION-COMMENT
1.	Massachusetts Institute of Technology Man Vehicle Laboratory, Cambridge, MA Horizontal; Round Steel Rails; Carriage on Linear Steel Ball Bearings; Tensioned, Wrapped, Steel Cable Drive.	Comprehensive Series of Dynamic Measurements* Obtained, Definitive Data for Responses and Transient Effects.
2.	NASA, JSC, Houston, TX Life Sciences Laboratory Horizontal; Round Steel Rails; Carriage on Linear Plastic Ball Bearings; Tensioned, Wrapped, Steel Cable Drive.	Engineering Copy of MIT Sled. Series of Dynamic Measurements Obtained on Incompleted Sled.*
3.	European Space Agency Research Technical Center, Noordwijk, Netherlands Horizontal; Flat Metal Rails; Carriage on Opposed Wheels; Tensioned, Wrapped, Steel Cable Drive.	Sled Intended for Flight in Long Module Spacelab. Acceptance Test Report Data Reviewed in Comparison with Measurements From MIT
4.	Royal Air Force Institute of Aviation Medicine, Farnborough, UK Vertical; Hydraulic Driven Platform	New Facility, Review of Operating Test Data.
5.	National Center for Scientific Research Neuro-psychology Laboratory, Paris, France Horizontal; Carriage on Conventional Bearings; Linear Induction Motor Drive.	No Published Description of Facility. No Action.

* Instrumentation consisted of crystal type accelerometers with a 2×10^{-5}g threshold of sensitivity; data recorded and processed on a standard-to-industry dynamic analyzer.

4.1.1 MIT Sled and Test System Configuration

The general configuration for the MIT Sled is shown by figure 4-1. At the time of the measurements the sled was configured to apply an acceleration profile to a seated human subject with the acceleration direction in the Y-Y axis (through the ears). The sled included structural supporting members to carry experiment fixtures which enclosed the head of the test subject. The carriage rides on three-quarter circle precision linear ball bearings and travels along a set of precision-ground, hard-polished, steel rounds as rails 6.4m long and 2.54cm diameter. The rails have continuous support from the base structure. The drive cable was statically tensioned to 4000N and required 4 complete wraps around the driving sheave to assure transmittal of the acceleration forces. As a consequence, the driving segment of the cable moves across the drive sheave in relation to the position of the carriage along the rails. Therefore, the driving force applied to the carriage deflects through a small angle as the carriage moves along the rails.

The measurement sequence involved operations with the cables disconnected (movement by hand), operations with the drive system unpowered and operations with power from the driving motor with control of the force profile provided by means of a function generator (a practical consideration used for implementing the acceleration profiles pertinent to the evaluation of acceleration noise).

4.1.2 Measurement of Friction and Bearing Related Forces

The evaluation of friction forces and bearing related effects began with individual measurements on the carriage and drive system. The carriage was disconnected from the drive cables and nudged into motion with a human subject aboard; figure 4-2 shows the force profile to overcome the static

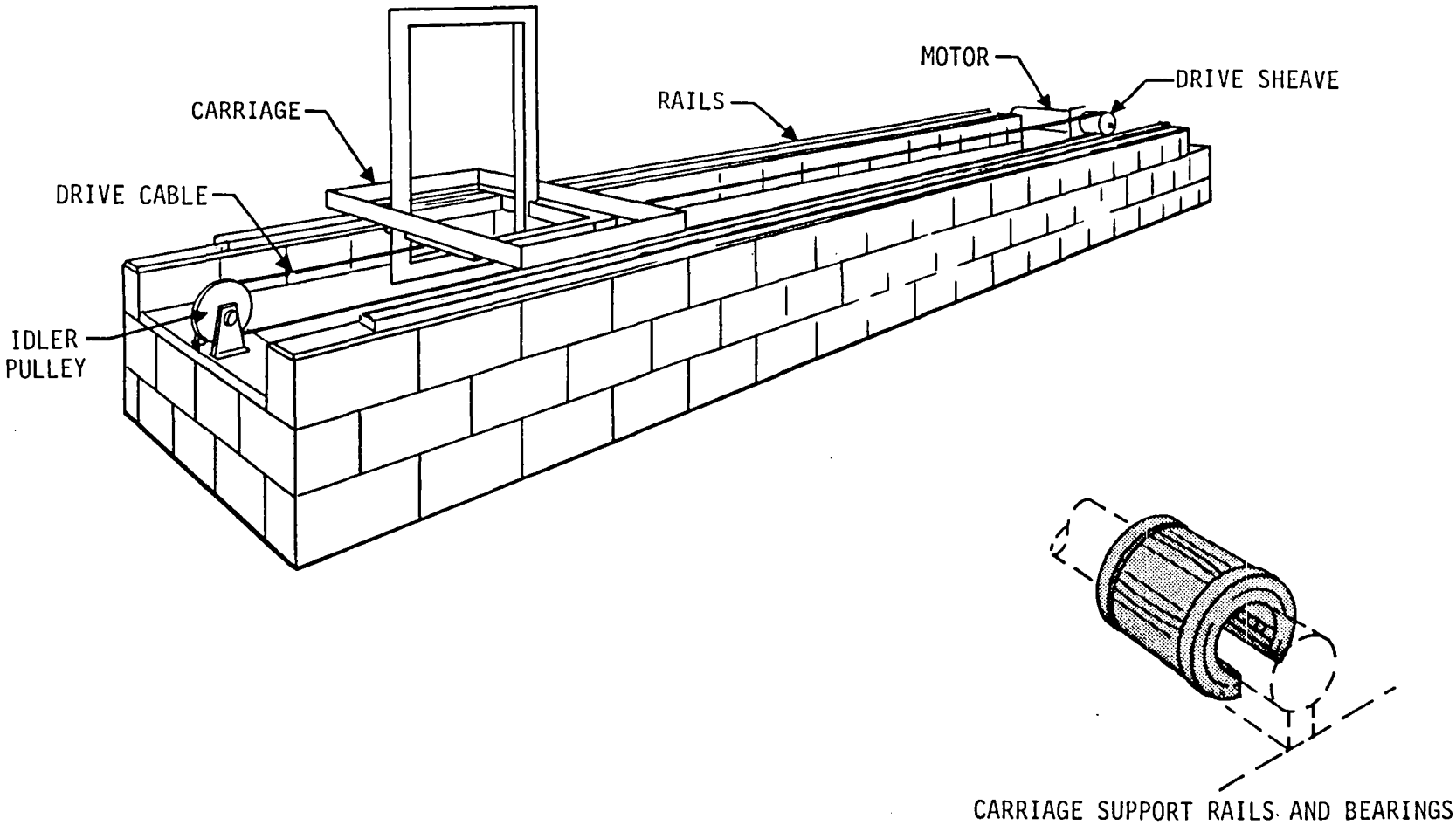

Figure 4-1. General Configuration of the MIT Vestibular Research Sled

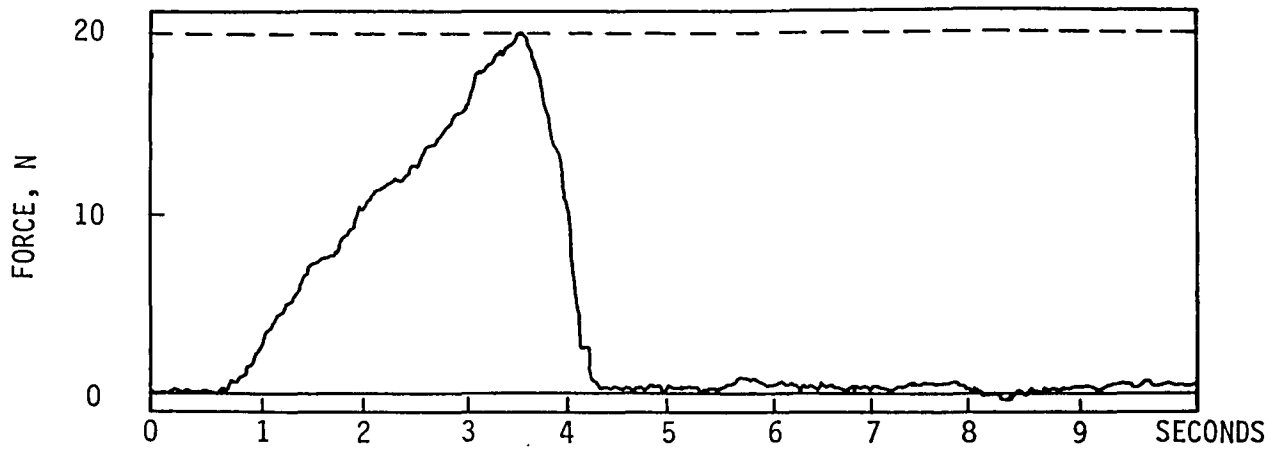

Figure 4-2. Force to Overcome Static Friction in Carriage Support Bearings

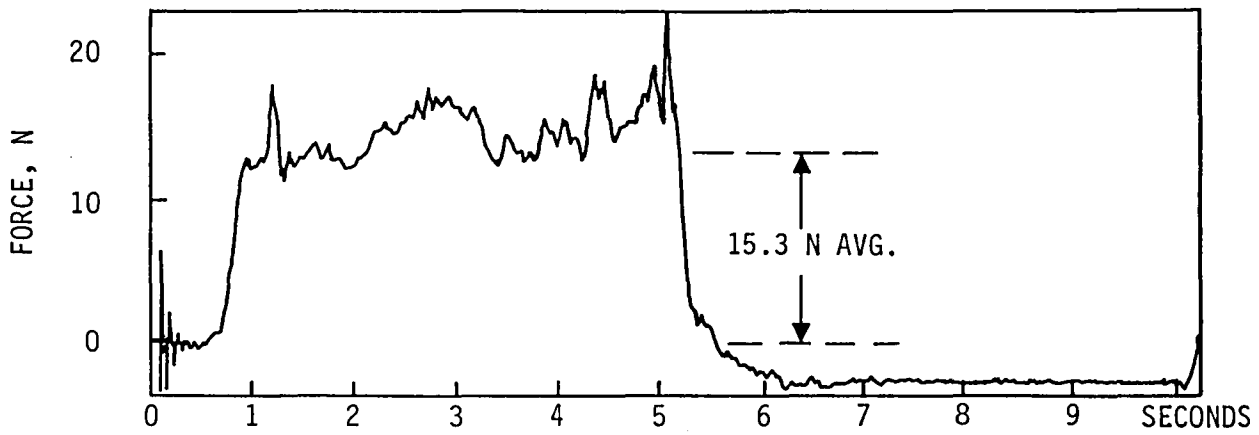

Figure 4-3. Force to Rotate the Drive Sheave 720 Degrees

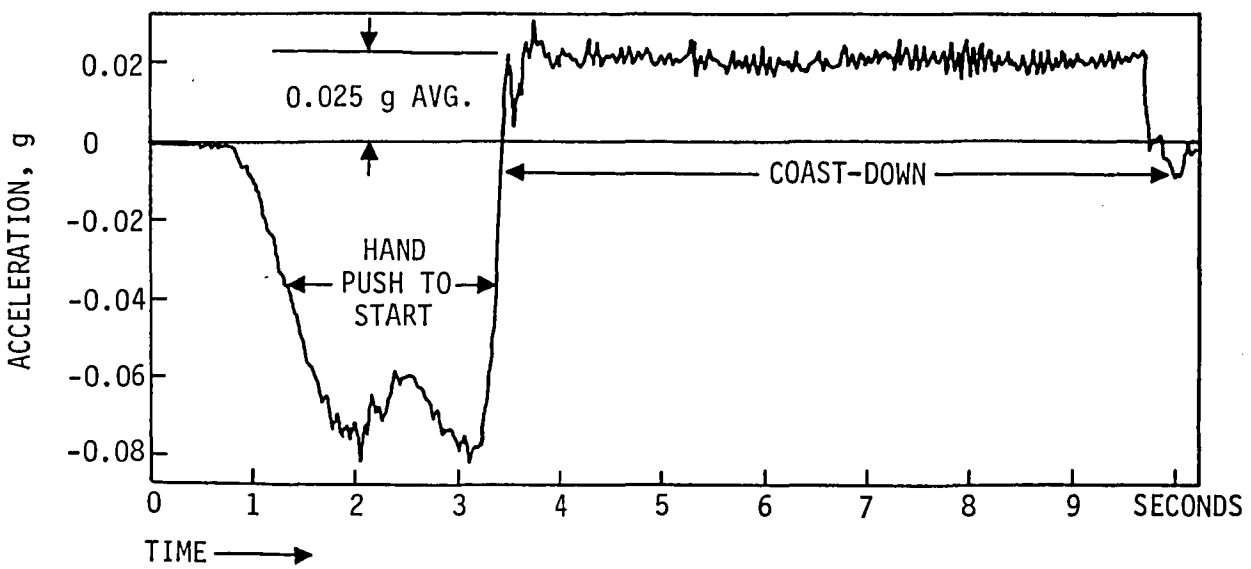

Figure 4-4. Coasting Acceleration from Bearing and Cable Friction

friction of the four linear ball bearings. At the breakaway from static friction, the force amounted to 20N. A force measurement by pulling on the drive sheave showed a friction force of 15.3N; figure 4-3 shows the force-time profile to complete two revolutions of the drive sheave. This force represents the bearing drag within the motor as it would be sensed by the carriage (motor leads disconnected, no electrical drag). The combination of the two effects predicts a coast down acceleration of 0.023g for the total system. A coast-down measurement with the drive cables in-place and tensioned appears in figure 4-4 and shows a drag force of 0.025g. The agreement is considered good since the total system includes some loss due to the bearings in the idler pulley and flexing in the cable. The friction coast-down drag plus the effect of electrical dynamic braking were measured by accelerating the empty carriage to about 1 m/sec (0.2g for 0.5 sec) and allowing the system to coast to a stop. The motion showed a friction and dynamic braking drag essentially proportional to velocity and independent of either the location on the track or the direction of motion. Figure 4-5A, B and C show the force profiles recorded. The abrupt stop represents the effect of static friction. The indicated value of 0.04g as the step at the end of the coasting deceleration for an unloaded carriage agrees with the 0.025g measured for the coasting case with a human subject aboard.

These measurements indicated that static friction effects at the zero velocity point could produce a detectable cue. The effect was confirmed by operation; figure 4-6 shows the responses measured with a human subject on the carriage subjected to alternating square-wave accelerations of 0.02g applied for 5 seconds. A bump transient occurs at the midpoint in each of the accelerations and corresponds to the zero velocity point for the carriage. The data shows a reversal transient of ± 0.01g maximum amplitude

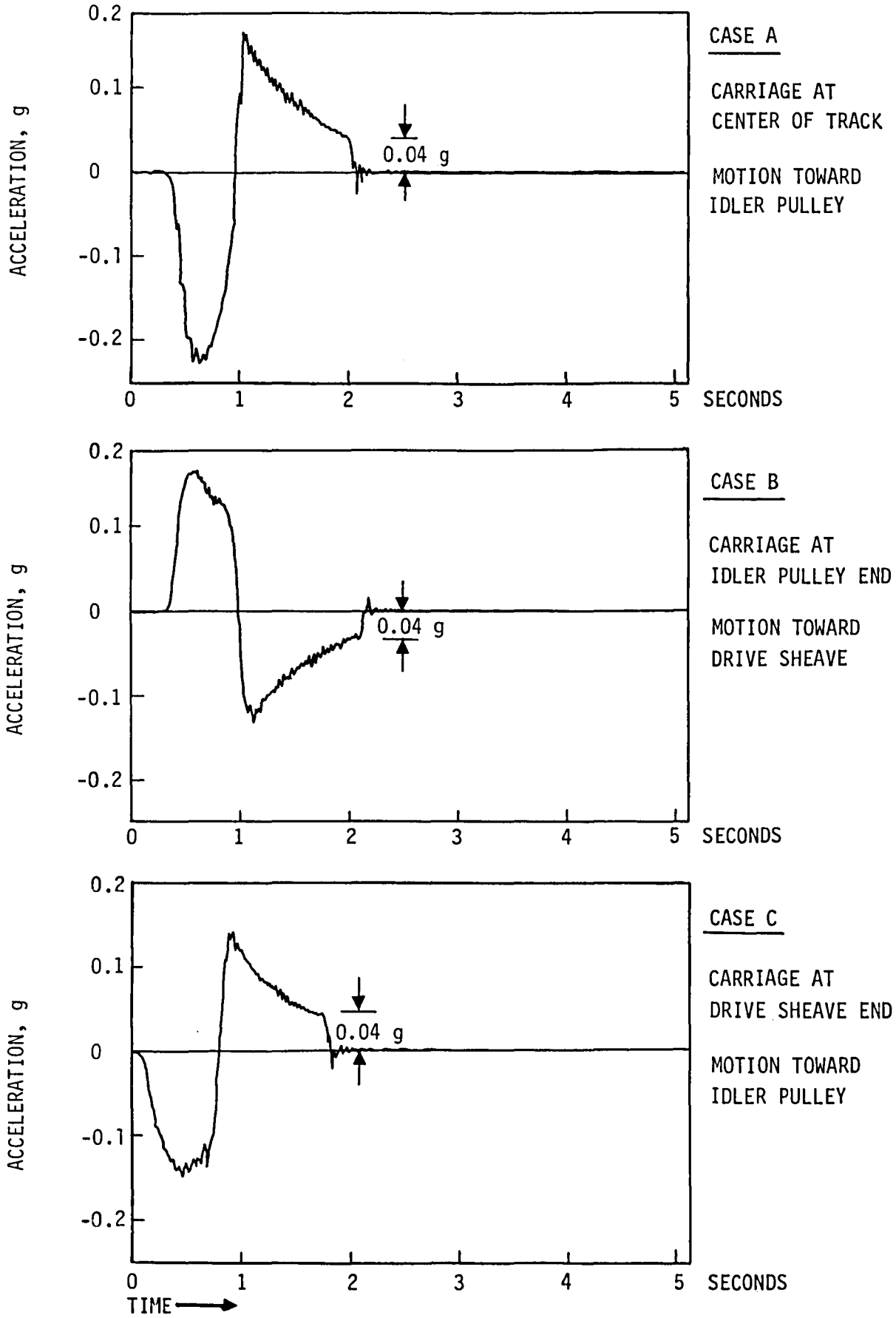

Figure 4-5. Coast-Down With Bearing and Cable Friction Plus Motor Dynamic Braking

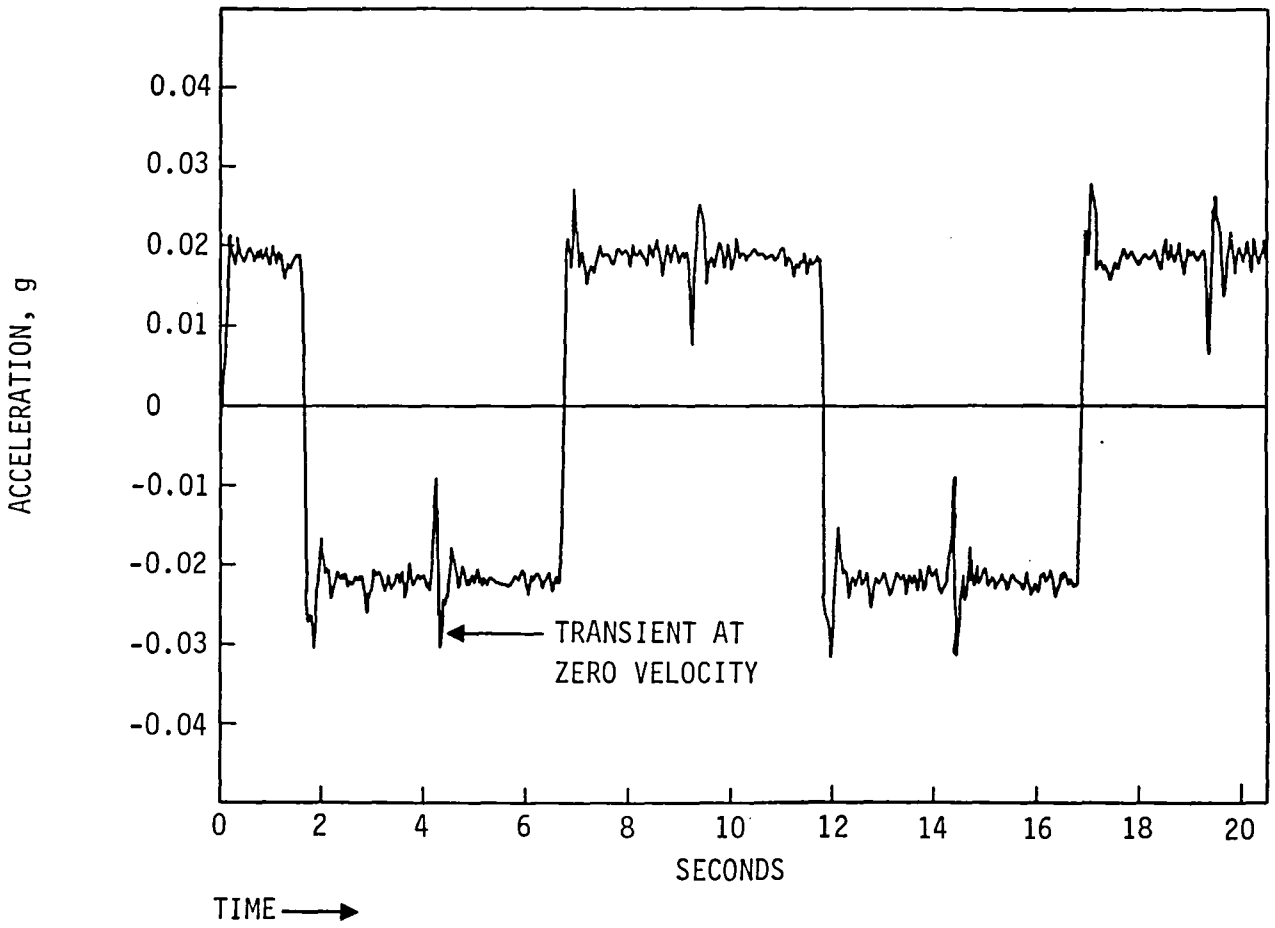

Figure 4-6. Acceleration Responses to Alternating Constant Accelerations

occurring over a period of 0.2 seconds (5 Hz); the test subject sensed the transient. There is some evidence of a higher peak for this transient corresponding to a higher frequency however 0.01g is well above measured thresholds-of-perception at 5 Hz (see figure 3-1, Data Points 13, 17).

These measurements and results confirm the technical difficulties presented by static friction in bearings to a system which has to apply oscillating motion without acceleration cues. On the other hand, once static friction has been broken, the drag forces are relatively small and constant; the bearings and drives utilized in this system do not compromise any measurements involving continuous accelerations or continuous motion.

4.1.3 Drive Cable Related Effects

The tensioned drive cable has the capability to introduce vibrations into the carriage as it moves along the track. Each of the three elements of cable span represents a potential vibration frequency defined in terms of the span length, the tension applied and the material properties of the cable. Two of these frequencies are related to the position of the carriage along the track. The evaluation for cable-induced noises consisted of vibration measurements on an unoccupied carriage while it moved at constant velocities of 0.1m/sec and 0.5m/sec. In both cases the carriage showed a complex-wave vibratory response. At a velocity of 0.1m/sec, the response was approximately 0.002grms. For a velocity of 0.5m/sec, the vibration showed a linear increase to 0.01grms. A spectral content analysis for the vibration at 0.1m/sec appears as figure 4-7 and does show a number of response peaks. The major peak near 12 Hz correlates with the predicted vibrating-string fundamental for the 6.4 meter length of cable between the drive sheave and the idler pulley.

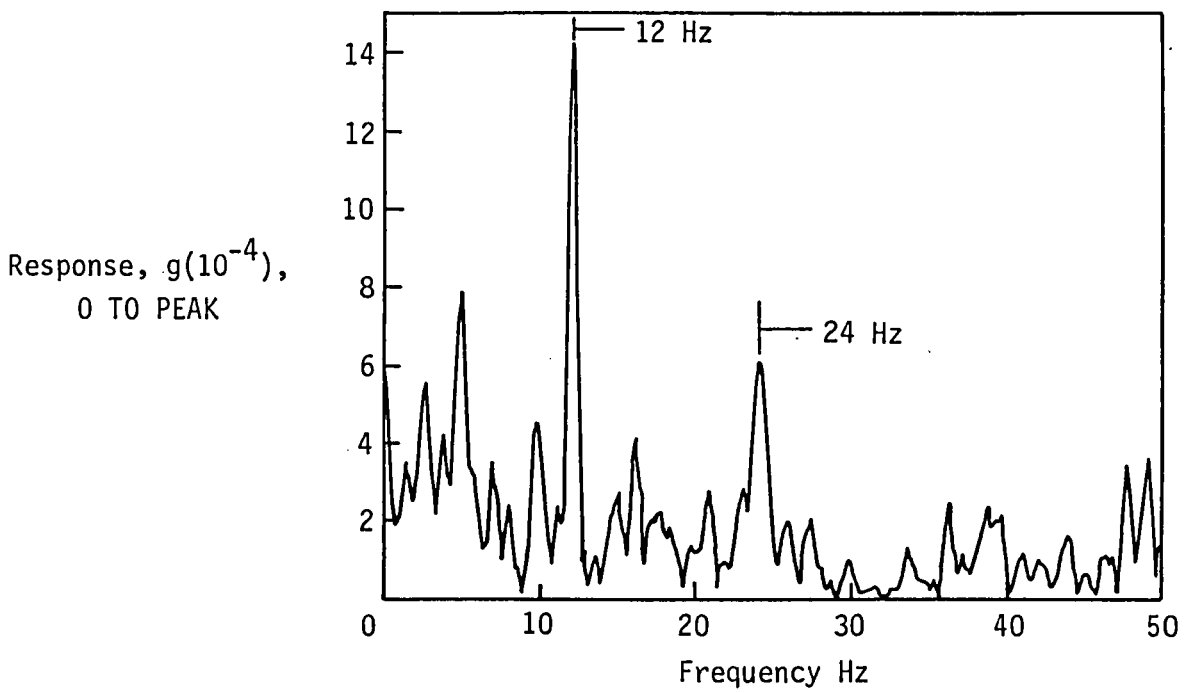

Figure 4-7. Frequency Spectrum for 0.1 m/sec

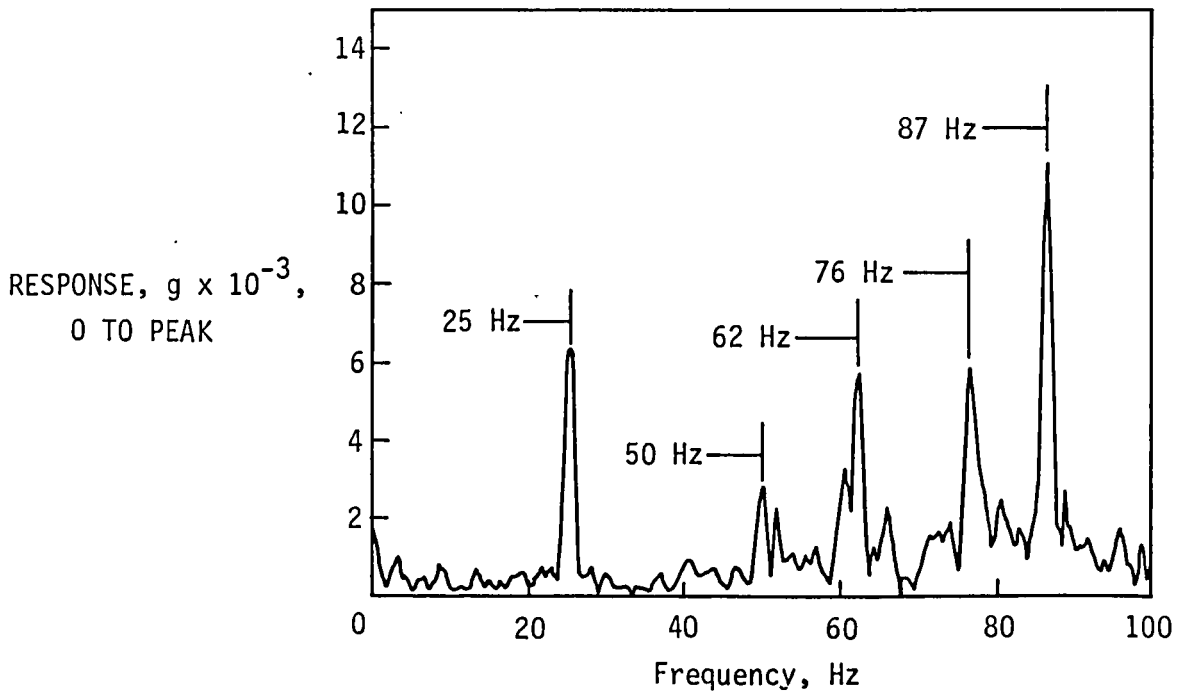

Figure 4-8. Frequency Spectrum for 0.5 m/sec

The other higher peak (e.g., 24 Hz) could be an harmonic or the combination of two near-equal cable resonances corresponding to a half-stroke position for the carriage. (The 10 second run for the spectral analysis involved about 1 meter of travel near mid-stroke.) The companion measurement performed at 0.5m/sec (figure 4-8) shows a pattern of discrete frequency peaks out to nearly 100 Hz; cable harmonics can account for some of the frequencies. The peaks show magnitudes 3 to 5 times greater than those measured at the lower velocity, and these peaks begin to approach the measured values for thresholds at their frequencies (see figure 3-1, Data Points 11, 13).

Wrapped cable drive systems with static tension will excite vibration due to the inherent geometry of the configuration; figure 4-9 shows the two sources of vibratory excitation. A wrapped sheave (figure 4-9A) driving a tensioned cable forces a small angular bend at the points of entry and exit. The combination of cable twist and side force against the groove in the sheave produces a condition relatable to a continuous "bowing" with a rough edge. In both this case and its musical equivalent, the result is vibrating "noise". Wire rope has an inherent resistance to bending, the individual strands have to move relative to each other to accommodate the difference in wrap-length around a sheave. In the case of the tensioned cable drive, these friction-hysteresis effects change sign coincident with the reversal of motion. The net effect is an impulse which serves to excite vibrations and can also appear as an acceleration cue to a test subject (see figure 4-6).

Thus, the application of tensioned, wrapped wire-rope cables to drive systems has to recognize an inherent condition for causing vibratory excitations. Vibration free operation cannot be reasonably expected. For

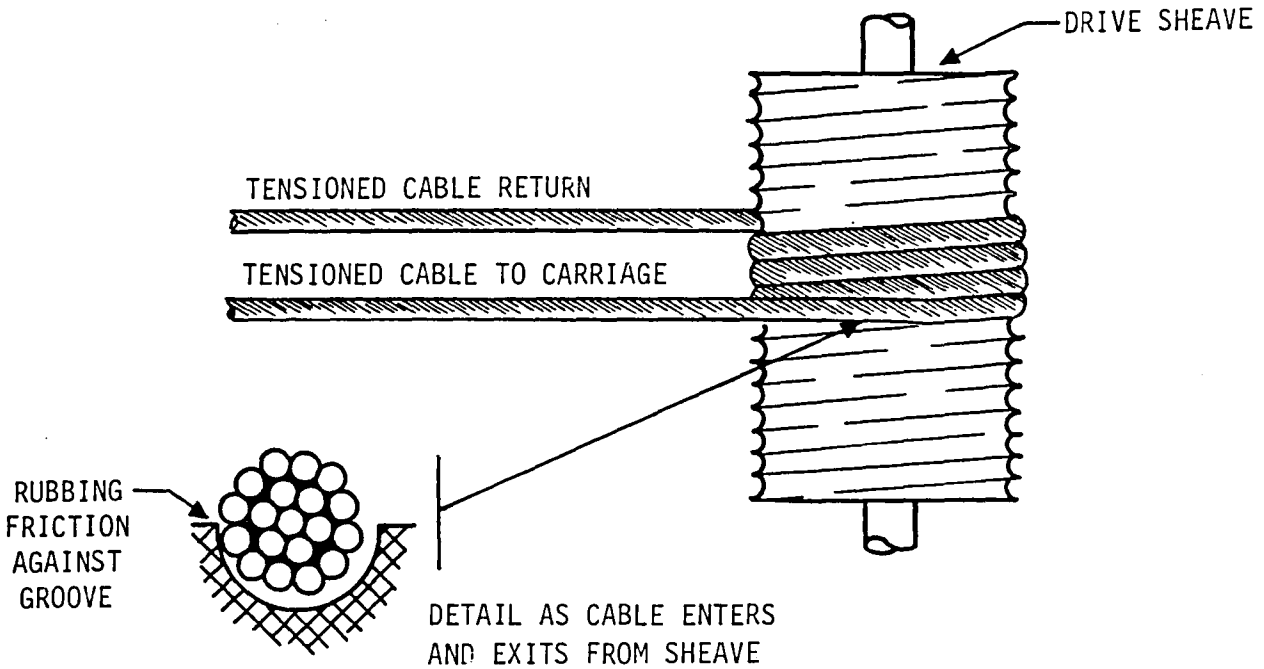

A. RUBBING FRICTION IN CABLE DRIVE

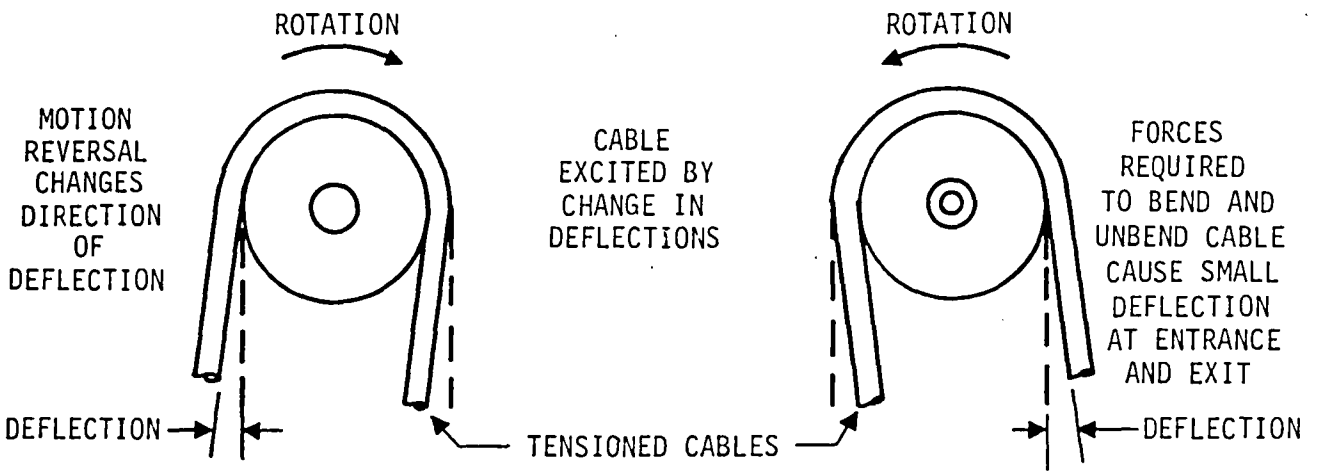

B. BENDING FRICTION AT CABLE DRIVES AND PULLEYS

Figure 4-9. Cable Related Friction Effects

man-rated equipment, the impulse transient coincident with motion reversal presents a technical compromise which has no obvious means for elimination.

4.1.4 Other Noises

The operation of the sled was evaluated for acceleration noises transmitted through structure and acceleration noises generated from other sources in the system. Such effects would be a concern if they correlated with the motion. An effective evaluation of sled-originated noise had to be assured that building responses and other environmentally applied excitations were eliminated either as a source or by extraction from the data. Building and environmental effects appeared negligible and not correlated with the motion. Figure 4-10 shows the background excitations present at the sled. All these excitations are considered compatible with the design limit shown in figure 3-1. In observation, a degree of care in the location and construction of the foundation elements can eliminate a potential source of extraneous noise. The operation of the sled showed vertical excitations with peaks ranging from 0.001g to 0.03g. Figure 4-11 shows the response content at the point of support for the test subject, however, these resonances do not provide any cues to the test subject. An additional structural resonance at 25 Hz appeared to exist between the input to the test subject and the mounting point for the head enclosure. Measurements in the horizontal direction perpendicular to the direction of motion appeared less than 0.001g and were considered negligible. The evaluation showed that the carriage as an element of the system did not have resonances or noises which were considered significant contributors to the total noise content or to the generation of acceleration cues. In assessing these measurements, it appears that the design of a carriage should be governed by frequency criteria (figure 3-1) as the means to avoid generating any extraneous sources for acceleration cues.

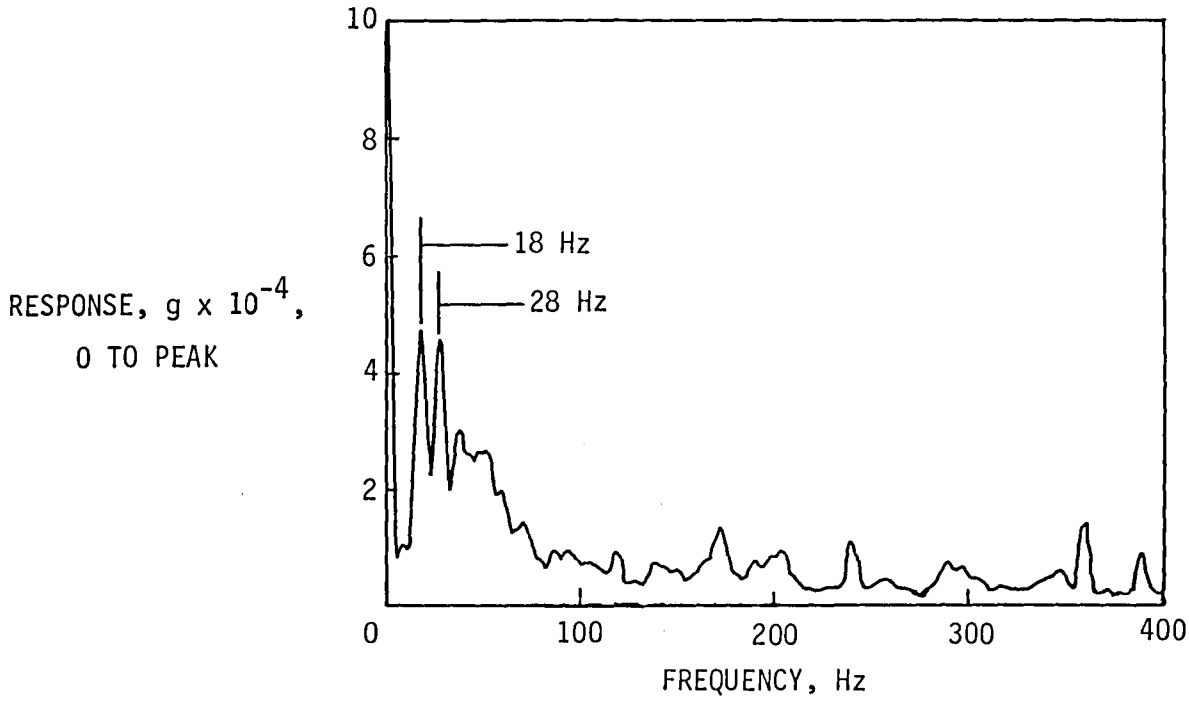

Figure 4-10. Building Vibrations Into the Sled Foundations

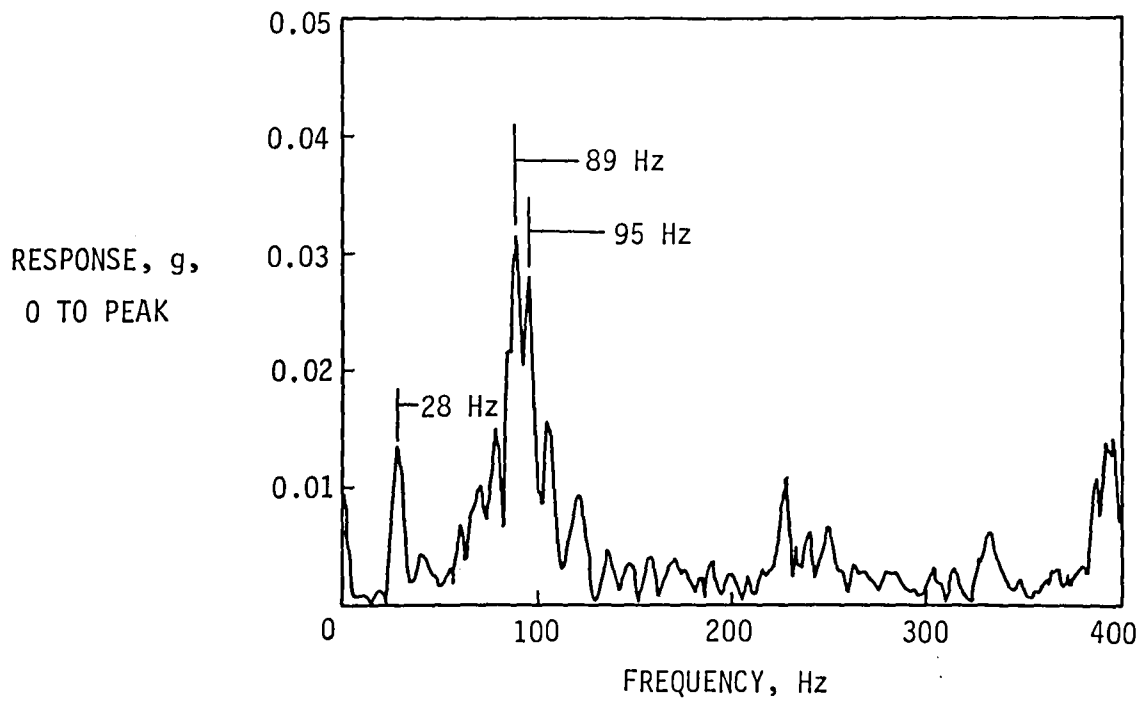

Figure 4-11. Vibration Responses in the Vertical Direction For a Moving Carriage

4.2 Measurements From the JSC Sled

The acceleration test sled at the NASA JSC is an engineering copy of the unit installed at MIT. The principle modifications introduced were the use of plastic balls in the bearings and 5.1 cm diameter precision steel rounds for the rails. The sled was not completed at the time of the measurement, the drive system employed an interim 60 Hz supply instead of the 2kHz unit intended. The measurements were intended as pathfinders and addressed structural resonances, drive system effects, friction effects and ride quality. The principal findings are summarized in Table 4-2 below.

TABLE 4-2. SUMMARY OF MEASUREMENT RESULTS AT JSC

Parameter	Measurement or Result
Structural Resonances	Carriage, 37 Hz Lowest. Principal Resonances at 151 Hz and 202 Hz
Cable Drive Resonances	7.75 Hz Fundamental Plus Harmonics
Overall Coefficient of Friction	0.03
Contribution From Rails and Bearings	0.02
Contribution From Cable and Drive	0.01
Other Effects	Motor Harmonics of 60 Hz up to 180 Hz

The ride quality measurements showed contributions from the carriage at 37 Hz, the cable at 7.75 Hz, plus the motor harmonics. The 60 Hz harmonics disappeared with the installation of the 2kHz supply. A friction coefficient of 0.03 during motion reversal generates the same value of acceleration force expressed in terms of "g" and such levels are above most of the measured thresholds of perception.

4.3 Review of the ESA Sled Acceptance Test Data

The ESA acceleration test sled was configured for compatibility with a long module Spacelab installation in the Shuttle. The principal dimensional constraints were the 5.4m length and 0.6m width. The drive system utilizes a tensioned, wrapped cable to move a carriage riding on four sets of opposed wheels. Each wheel turns in a pair of radial ball bearings at the axle support. The description and data from the acceptance testing (ref. 6) show evidence of non-linear friction effects coincident with the times of motion reversal for the carriage. Figure 4-12 shows the acceleration and velocity measurements obtained from the carriage for operation at a 0.2 Hz cyclic application of 0.01g accelerations. The response measurements show an acceleration-interrupt coincident with zero velocity which approximates an 0.008 g half sine at 0.75 Hz. The velocity trace shows a corresponding hesitation at each zero crossing. These responses are above perception thresholds. The further analysis of the data estimates 0.02g as the measured maximum for the reversal-transient effect. These measurements are the summation of static friction plus the reversal of running friction. The frequency and magnitude of the response are functions of the servo response characteristics coupled with the elasticity of the cable drive and structure up to the point of the measurement location.

4.4 Review of Description, RAF Vertical Oscillating System

The measurements from tests and description of the design for a "large-stroke oscillator" installed in an RAF research laboratory indicates a system which will operate without presenting spurious acceleration cues to the test subject. The hydraulically driven unit operates in the vertical direction to provide strokes up to 2 meters over the frequency range 0.05 Hz to 30 Hz and at sinusoidal excitation levels ranging from 0.001g to 3.0g into

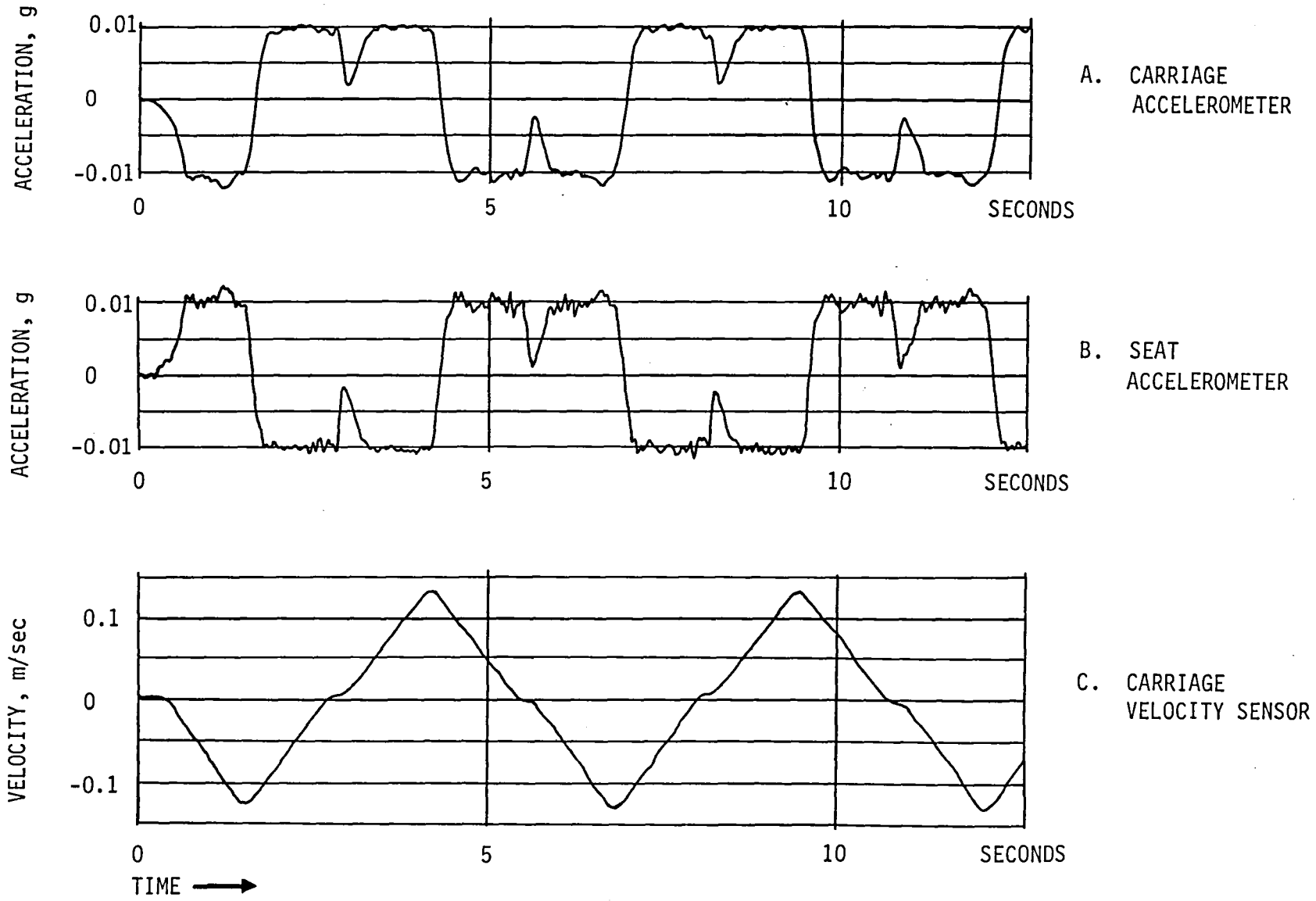

Figure 4-12. Measured Responses from the ESA Sled.

a test load of 200 kg. The design of the control system and the innovative application of hydraulics resulted in data which to quote the evaluators "revealed a commendable waveform fidelity and low spurious noise." The analysis of data showed that for measurements in the threshold range (0.01g) spurious excitation content was of the order 0.001g. These values are consistent with elimination of acceleration cues.

The design of the system employs continuous flowing hydraulics and a pneumatic balance of the gravity force to achieve the noise-free operation; figure 4-13 shows the general configuration. The features which serve to eliminate spurious noise at reversals of motion are:

1. The plenum chamber at the bottom operates at a pressure ($\backsim$ 3 times atmosphere) sufficient to balance the gravity load of the column, platform and test subject. The plenum volume does not experience an appreciable change throughout the length of the stroke.
2. The upper and lower bearings for the column utilize a radial inflow of hydraulic fluid to center the column and prevent any mechanical contact or drag forces. (Hydraulic fluid continuously weeps into the plenum and is continuously scavenged from around the top bushing.)
3. The piston does not contact the walls; the side faces of the piston have conical reliefs from each end toward the middle such that the hydraulic fluid moves along a tapering passage to produce a centering action. There is a continuous fluid flow; the piston has bleed holes in the middle face and fluid exhausts into the hollow column and, thereby, to the plenum for recirculation.

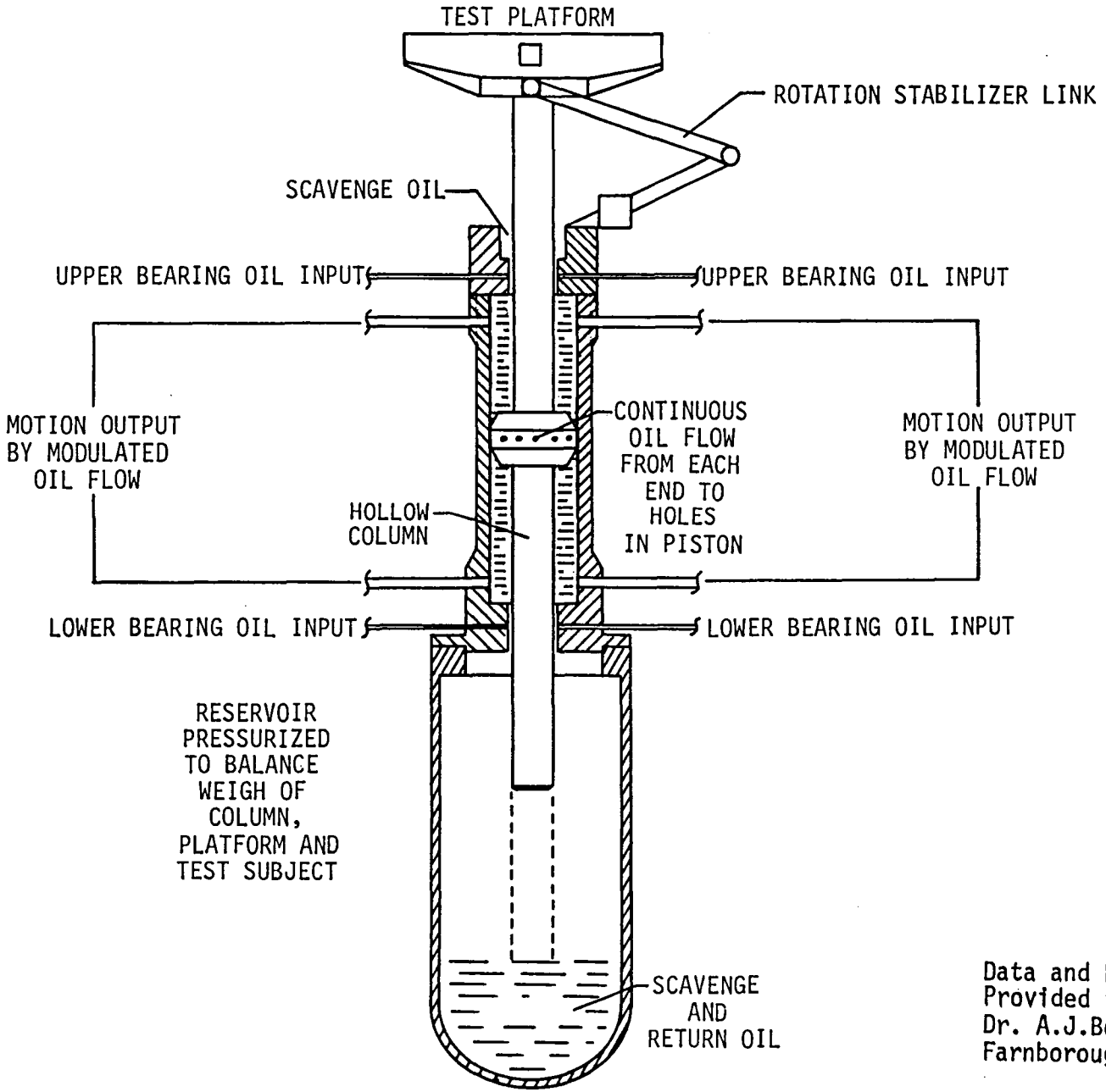

Figure 4-13. Vertical Motion Test Platform at the RAF Laboratories,

The concept eliminates those elements which tend to generate hysteresis forces during a motion reversal. The reversal of the driving forces is achieved by modulating the flow of fluid; however, such changes occur at the time of maximum kinetic energy in the moving elements, and thereby minimize any perturbing effects. The installation represents a large national facility and long-stroke hydraulic systems do not appear compatible with flight. (The diameter of the column is listed as 200mm and the operation requires a 160 kw hydraulic system.)

4.5 Summary of Findings From Sleds

The summary of measurements and reviews of published results show that systems can be configured which will operate without spurious acceleration cues above the thresholds of perception. On the other hand, sled carriages riding on conventional bearings will experience a non-linear friction effect coincident with reversal of motion. The measured levels for high quality bearings show typical values of 0.02g which is above most of the measured thresholds for perception. The use of a tensioned, wrapped wire-rope cable to impart the accelerating force must contend with resonance vibrations associated with the free-string length of the cable runs and continuous vibratory excitations. The use of tensioned wire rope also introduced a measurable hysteresis effect stemming from flexing-induced friction. Cable and drive system hysteresis can apply forces of 0.01g to a carriage during a motion reversal. Careful design can minimize the effects, however no obvious means has appeared which will reduce the effects to levels below perception thresholds for a system based upon conventional bearings and driven by a wire rope.

5.0 EVALUATION OF TECHNOLOGY FOR APPLICATION TO LOW NOISE SLEDS

The measurements of static and dynamic friction forces in existing mechanical sleds showed that the levels were too high and produced acceleration cues well above perception limits. Methods of lowering these effects were investigated. Some of these were the use of wheels with large wheel-diameter to bearing-diameter ratios, wheels supported by belt-constraints (no bearings) and air bearings. Air bearings appeared clearly superior, the friction levels are negligible, and the disturbing torques are below perception limits. Evaluations of alternatives to the tensioned, wrapped wire rope drive appeared as an application of linear induction motors and as metal belts running on air bearing supported pulleys. The evaluations which are described below indicate that a low noise sled acceptable to both ground and flight operation appears achievable. The sled would utilize air bearings to support the carriage and employ a drive system based upon a linear induction motor or as an alternate a flat metal belt. A drive system utilizing metal belts also would need to employ air bearings for all of the pulley and tensioning elements.

5.1 Air Bearing Systems

Air bearing devices are well understood, covered in detail in many texts, and are widely applied to existing mechanical equipment. Two commercial systems were investigated as to noise level, availability, and cost. One commercial bearing element was investigated regarding its potential use as a linear motion constraint for a Shuttle mid-deck experiment. The characteristics of these devices are described in the following paragraphs. The data gathered ranged up to 400 Hz, however, only the results below about 100 Hz are of concern. Shock mounts or foam pads are considered effective isolators for vibrations above 100 Hz.

The airflow required to support a test subject on earth and in the Shuttle environment was also investigated. A computation for worst case conditions evaluated support pads requiring differential pressure of 6.89 x 10^5 Pa (100 psi). For 10 pads, each using 0.00425m^3/sec the overall requirement was less than 165 watts. The actual requirements in a Shuttle environment should be smaller because the air bearing pads would only carry moment loads and not have to support the carriage, chair and subject. Residual thrusts caused by the air exhausting from the pads were also computed and found to be negligible. The largest disturbing torques which could be encountered are those which may be caused by angular inclinations of the support pad. The disturbing angular accelerations are directly proportional to the inclination of the pad. To achieve torques which produce lower than perception level accelerations it is necessary to provide the support pads with a self-aligning capability. Angular misalignments must be kept below 0.0003 radians in the direction of the motion. These conditions present no difficulty with well-designed pads. In the commercial items evaluated, the overall bearing clearances were between 0.007mm and 0.015mm total, an angular misalignment of 0.0003 radians does not appear achievable.

5.1.1 Measurements and Evaluation of Performance for a Commercial Precision Measurement Unit

A precision coordinate measuring unit produced by a U.S. manufacturer has been installed as part of the inspection equipment inventory at the NASA Ames Research Center (ARC). This unit was instrumented to measure vibration and acceleration responses to provide typical characteristics. Units of similar design are available in standard platform sizes ranging from approximately 1 meter by 1 meter up to 3 meters by 6 meters. The unit installed at the ARC is based upon a granite slab 3 meters

long, 1.5 meters wide and 30 cm thick weighing 3800 kg. The unit is supported by isolation footings. The active portion of the measuring system utilizes a movable carriage weighing about 340 kg floated on air pads; figure 5-1 shows the general configuration of the unit. The individual air pads in this unit are hard-faced (air fed by drilled holes) 7.62cm squares.

The results from a series of measurements showed that the floor moves with a maximum amplitude of 0.0001g in the frequency range 22 Hz to 30 Hz, apparently in response to other local machinery. The slab moves with 6 degrees of freedom and does amplify the floor vibrations by factors as much as two. The carriage follows the motion of the slab to within 5×10^{-5}g at frequencies up to 100 Hz. Above 100 Hz the carriage shows additional response; figure 5-2 shows the measured responses. The linear deflections between the carriage and the slab remain below 0.15 micrometers; at all frequencies up to 400 Hz, these levels are small and can be readily attenuated. The results from these measurements conclusively showed that the noise levels associated with air bearings remain below the design limit defined for thresholds of perception avoidance in test equipment (ref. figure 3-1). In a follow-up discussion with the manufacturer, the cost quotations and times for delivery led to suggesting the use of these tables as one of the alternate test configurations described in the Appendix.

5.1.2 Evaluation of Air Bearing Pads Using Porous Metal

A comparison set of measurements were obtained from an alternate precision profile measuring unit which utilized air bearing pads formed from porous metal (air supply over the entire pad face area). Figure 5-3 shows a comparison of the slab vibrations with the responses measured on the carriage. The relative accelerations between the carriage and the supporting slab are less than 2×10^{-5}g at all frequencies up to 400 Hz. The porous metal

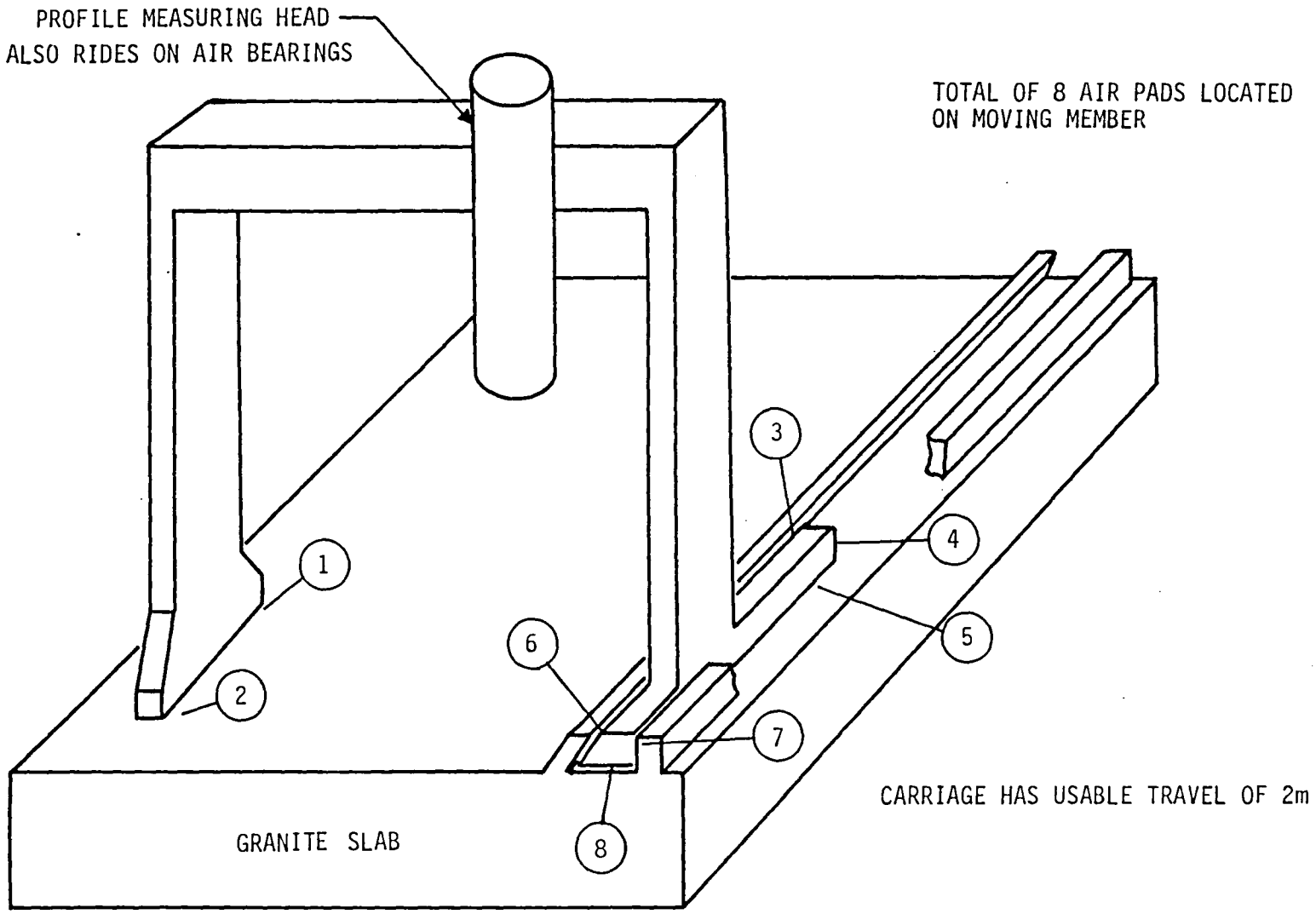

Figure 5-1. Commerial Profile Measuring System Using Air Bearings to Support Carriage

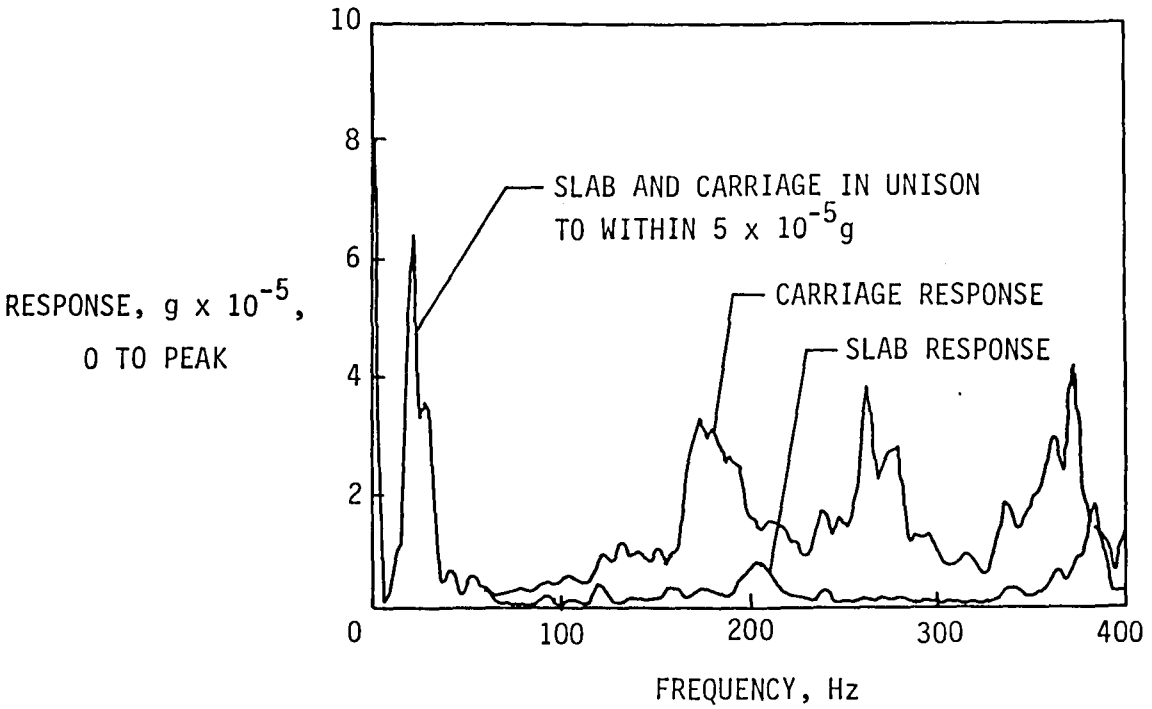

Figure 5-2. Vibration Responses for Hard-Faced Square Air Bearings

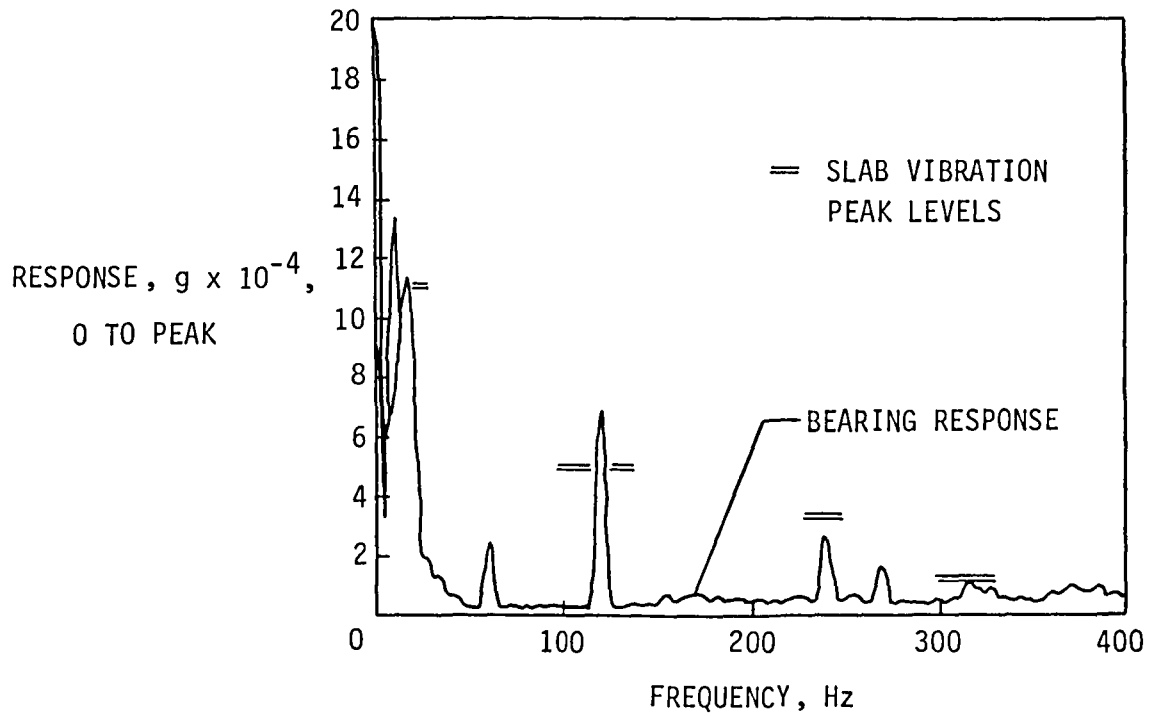

Figure 5-3. Vibration Responses for Porous Metal Faced Square Air Bearings

bearing faces appear to more closely follow the motion of the supporting slab than do hard-face units with discrete-feed holes. Attempts to measure the coefficients of static and sliding friction were not successful with either of the systems. The friction forces were below the 2×10^{-5}g sensitivity threshold for the accelerometers. These measurements indicate that an air bearing system will operate without any noise sources which could produce acceleration cues above the design limits shown in figure 3-1.

5.1.3 Other Configurations

A limited series of test measurements were obtained from a bearing configuration that included piston-type compensators which accommodate minor variations in the alignment of the supporting tracks. The single-pad configuration was tested under a load of 18.2 kg operating with supply pressures of 138000 Pa (20 psi) and 207000 Pa (30 psi). The measurements showed vibration levels less than 2.5×10^{-5}g for frequencies below 100 Hz.

The reviews of commercial air bearing data and available configurations led to the particular evaluation of a bearing-and-track unit which could be applied to a single-track sled configuration compatible with preliminary experiments conducted within the mid-deck of the Shuttle. Figure 5-4 shows the test concept. The air bearing and square-tube rail are a commercially available unit; the bearing element measures about 0.4m in length and would provide a stroke of 0.5 meters. The lightweight folding structure accommodates the test subject; springs or elastomers provide the drive system. When not in use (during launch, meals, and landing), the unit dismounts and folds for storage elsewhere in the cabin. The data supplied by the manufacturer shows the following test capability:

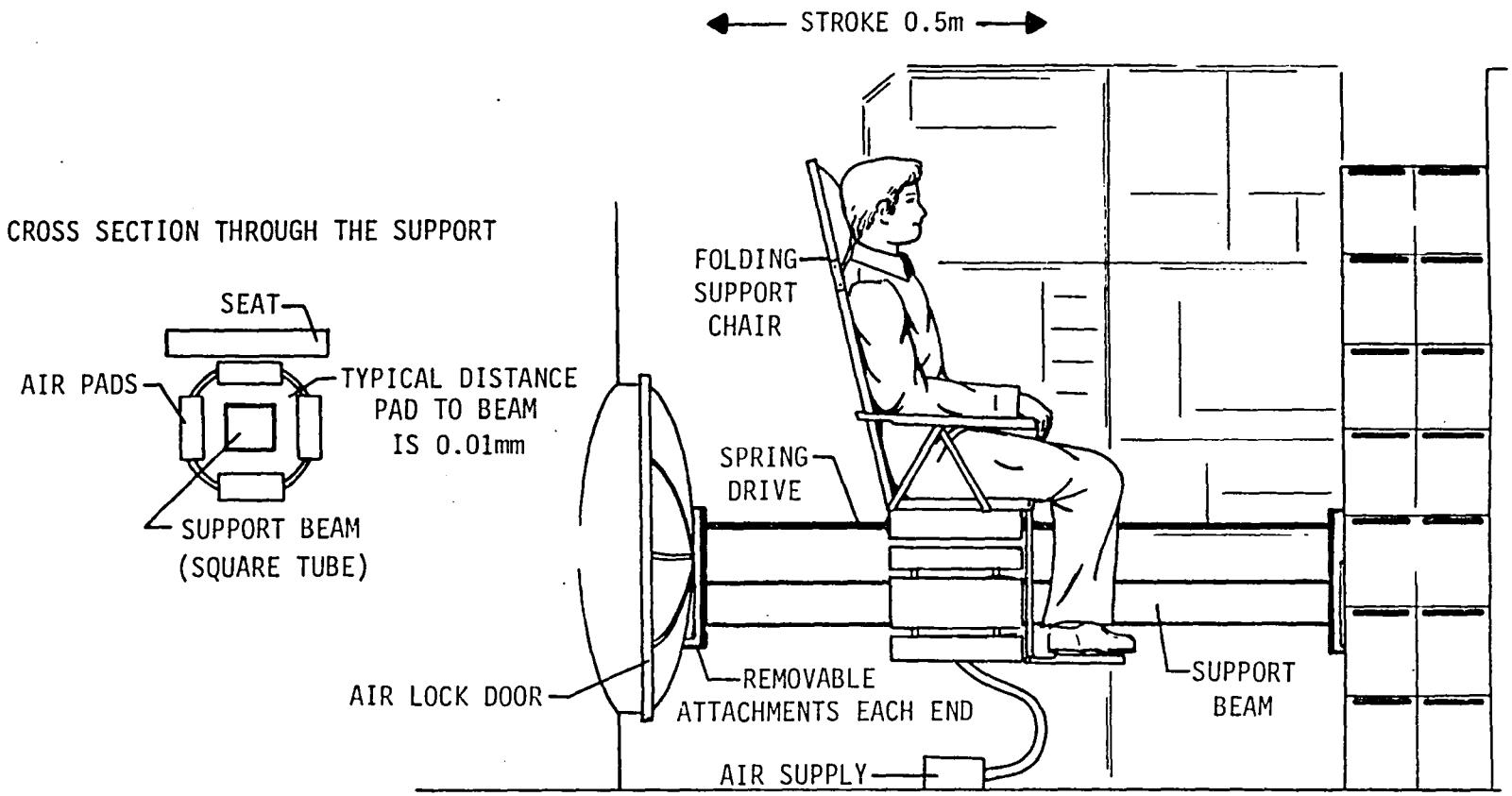

Figure 5-4. Concept For a Test in the Mid-Deck of the Shuttle Using a Single Air Bearing Support

Load	450 kg
Pitch Moment	62 Nm
Roll Moment	37 Nm
Air Supply Pressure	550,000 Pa
Compressor Delivered Flow	$0.00075 m^3/sec$
Compression Delivered Power	150 watts

The power requirements are within the capabilities of the Shuttle supplies; the air bearing units are catalog items with delivery times compatible with experiments-of-opportunity scheduling for the Shuttle.

5.1.4 Air Bearing Data Summary

The conclusions of the air bearing investigations show that the bearings are sufficiently noiseless to be used as sled supports, are commercially available, and that the compression horsepower required is reasonably small. The friction and disturbance torques introduced by the airflow are negligible. Therefore concepts for a sled which expects to keep acceleration noises below threshold of perception limits should consider air bearings as the available option.

5.2 Linear Induction Motors

Linear induction motors offer an attractive option for a low noise drive system. For application to a sled, the installation would take the general form as indicated in figure 5-5. The carriage would carry the moving coils and operate with a stationary reaction plate. The alternate configuration of electronically switched stationary coils and a moving reaction plate (armatures of ordinary electric motors are moving reaction members) could be employed in a ground test sled, however, practical considerations dictate that the coils contain iron, the weight penalty for non-moving coils appears incompatible with a flight sled. The theory and

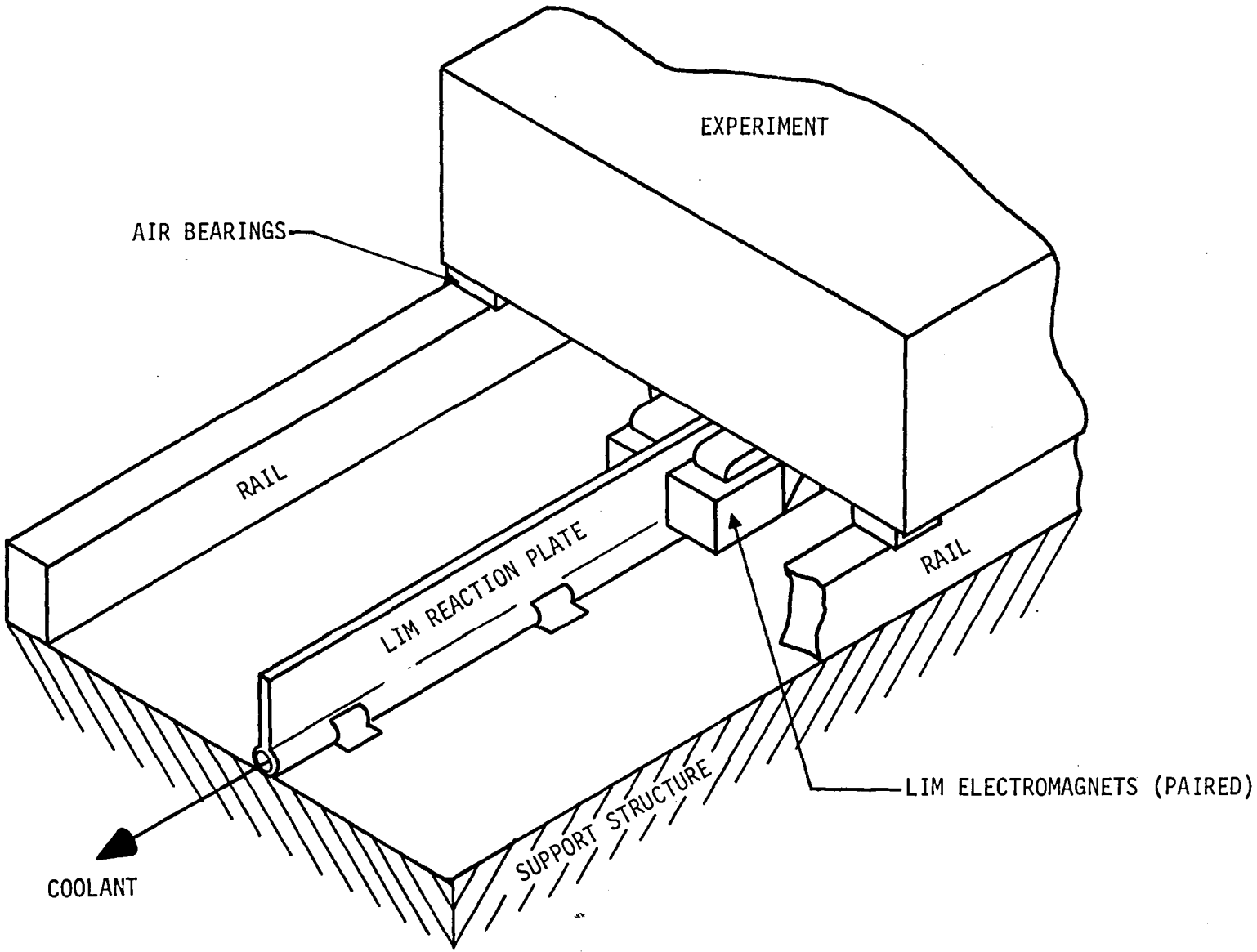

Figure 5-5. Linear Induction Motor Drive Concept

design of linear induction motors has been well established for industrial use (ref. 7) and no inherent problems have appeared which precludes their application to the drive system for a sled. The study into the application addressed some of the operating requirements as they relate to the electrical performance and the removal of heat. For discussion reference, the operating concept for a linear induction motor is presented in figure 5-6. The pole pieces of the motor follow conventional practice of coil-wound laminated iron. The reaction plate is a composite bar with an iron core surrounded by some readily coolable metal such as copper or aluminum. In operation, the individual pole pieces are energized by one of the phases of a multiphase electrical current (3 phase alternating current). The relative magnetization from pole-to-pole sets up countering magnetic fields within the reaction plate such that a net thrust will exist driving either the poles along the reaction plate (as in a sled) or the reaction plate along the poles (as in an industrial actuator system). In a three-phase system, interchanging the relative sequence of any two phases will change the direction of the thrust. In figure 5-6, if a 1-2-3 sequence causes a force in one direction then a 1-3-2 sequence will reverse the direction. The concerns for a drive system application become the relative efficiency in transferring electrical energy into thrust, the system for switching to achieve motion reversal and the ability to remove heat from the reaction plate since the electrical energy which does not appear as motion must be dissipated as heat.

5.2.1 Performance Efficiency

A linear induction motor applied to a sled drive will generally have to operate in a regime of low electrical efficiency. The need to operate at near-stall and to reverse thrust at maximum velocities (motor essentially driven backwards) diverge from the most efficient operating range

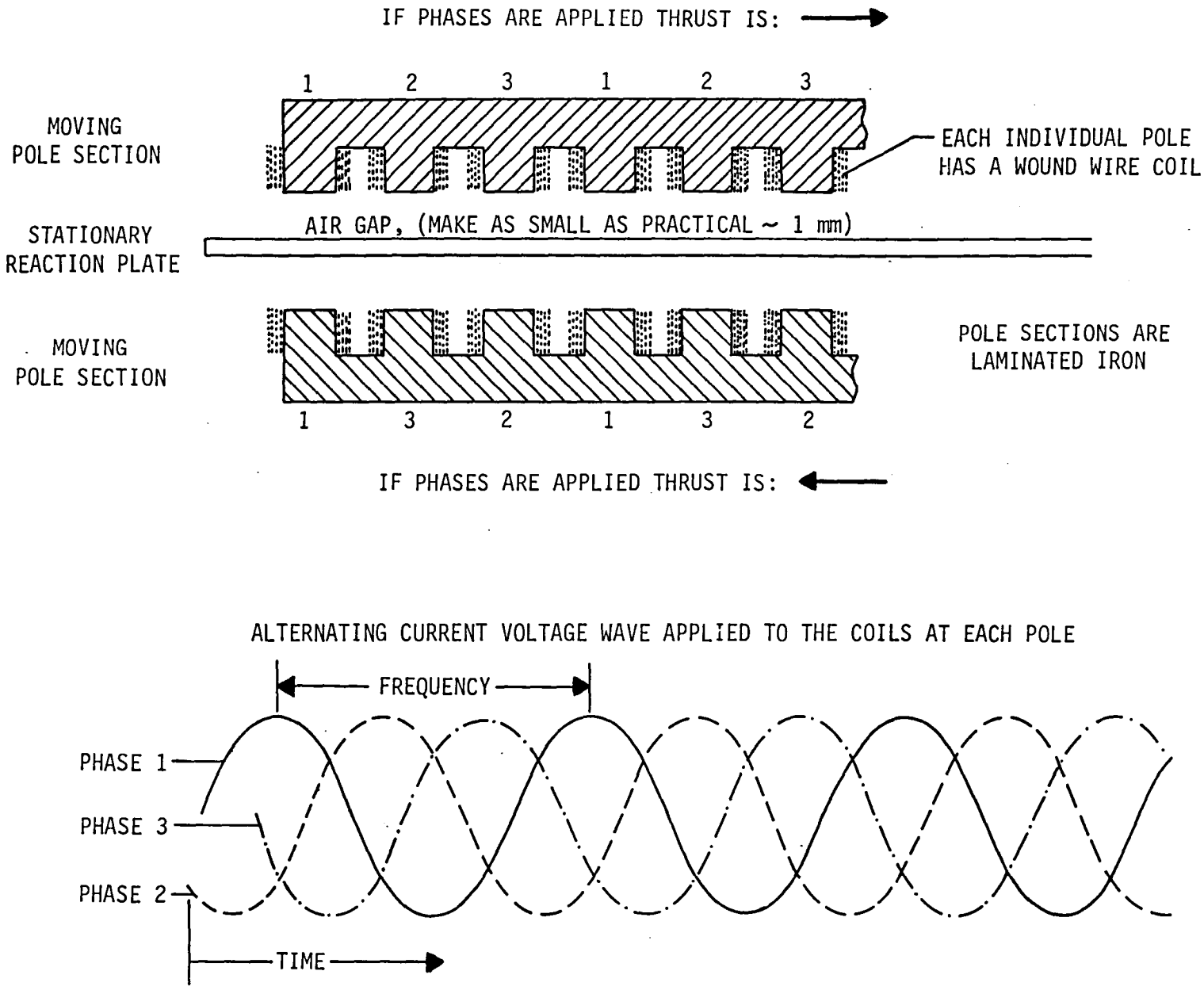

Figure 5-6. Operating Concept for a Linear Induction Motor

which relates to a sustained optimum velocity. As an example, for 60 Hz operation of a motor with poles on 5cm centers, the most efficient velocities occur above 5 meters per second; sled carriages are not expected to experience such velocities during ordinary operations.

A survey of present industrial units showed that a general rule equates 10 volt/amperes to 1 Newton of force. Industrial applications generally modulate the applied voltage as the means for controlling thrust, which is most effective since the thrust corresponds to the square of the applied voltage. While a thrust efficiency of 10 va/N appears acceptable for industry, an improved efficiency would benefit applications to sleds. Since all sled systems will need a voltage control and flight sleds would need a dedicated converter for the alternating current, the system could be designed for any frequency and this consideration offers a means to improve the efficiency. Studies performed by Laithwaite et al. in Britain (ref. 8) show that for operations near stall or at low velocities a lower frequency of alternation will improve the efficiency of the magnetic coupling which produces the thrust. A comparison evaluation is shown below as Table 5-1. The selection of 756N for the thrust generated represented an acceleration of 0.5g applied to a 150Kg carriage. The design of a moving coil system must accommodate the weight of the coils as part of the accelerating mass. Industrial specifications show that moving coil configurations can generate thrust forces up to twice the weight of the coils (e.g., a thrust-to-weight ratio of 2).

TABLE 5-1. COMPARISON OF OPERATING CAPABILITIES

Case	Hz	Max Volts	Watts Consumed	Thrust Generated N	v-a / N
1	60	300	10k	756	13.1
2	15	165	5.1k	756	6.74
3	5	150	3.4k	756	4.49

Case 1 represents actual measurements from a commercial unit operated at low velocities and through stall (motion reversal). The system efficiency degrades about 30 percent compared to operation at optimum velocities.

Case 2 represents an analytic prediction based upon both the measurements and the data developed in the low frequency evaluations (ref.8).

Case 3 represents practical lower limit for operation. A system configured for flight should consider the advantages offered by operating at the lowest practical frequency.

The requirements for reversing the direction of force dictate that the control system for the motor be capable of interchanging two of the phases applied to the coils. Fortunately, interchanges occur coincident with a zero force requirement. The techniques for zero-crossing switching have been developed for alternating current machinery. The configuration of the power control for a sled must include a high-speed switching technique that can accommodate the current requirements for the motor coils which may range from 10 to 50 amperes.

5.2.2 Cooling Requirements

The design of a linear induction motor which operates through a low-speed, high-force change in direction of motion must accommodate a heat dissipation in the reaction plate totaling 80 percent of the power applied. For the sled system evaluated, the cooling requirement became an 8000 watt dissipation from the reaction plate in the volume contained between the coils. Fortunately 8000 watts corresponds to a 20°C rise in a water flow

of 6 liters/minute. These flow rates in a cooling passage of 12.5mm diameter will keep the operating temperature of the reaction plate within ordinary acceptable limits. Cooling of the reaction plate and the coils does not appear to present any technical obstacles to the use of linear induction motors.

5.2.3 System Considerations

The use of a moving-coil linear induction motor coupled with air bearings for the sled carriage offers an attractive approach to a sled system which could be identical in both ground and flight configurations. The design of the sled system must address the need to have air hoses and electrical power leads connected to the carriage in such a manner they do not introduce an unwanted friction or drag effect. The concept of an auxiliary servo-carriage appears as an option. The second carriage would employ a follower servo which kept a close distance to the experimental carriage such that the power, air (and instrumentation) leads could make a short flexible connection between the two units. The drive for the auxiliary does not require either the power or noise isolation associated with the experiment carriage. In addition, the design of a sled system may want to include a moving cover (a roll-sock or bellows) to protect the precision rails from contamination or harm; a follower carriage would provide the means for extension or control of a protective cover.

5.3 Metal Belt Drives

Metal belts have well-developed applications to industrial operations particularly where precision transfer functions must be accomplished in an automated assembly or processing line. Metal belt materials are available in aluminum, steel and beryllium copper. The corrosion resistant "stainless" steels are well utilized in handling

materials moving through corrosive processes. In general the manufacture of metal belt materials focuses on the development of high tensile strength (through work hardening or heat treatment), the precise control of thickness and the production of high quality surfaces. In application to the drive system of a sled, the use of a wide (20-30cm), thin (0.05-0.4mm) belt would avoid most of the dynamic problems inherent with a tensioned, wrapped cable (e.g., resonance frequencies, flexing losses, sheave induced noises, etc.).

The evaluation of metal belts consisted of analytic studies of a steel belt which indicated that such a configuration can provide adequate force with less than one complete turn around the driving pulley. The analysis addressed the following potential sources of acceleration noise:

1. Friction losses caused by bending of the belt around the pulley.
2. Friction losses caused by partial slipping of the belt on the pulley.
3. Disturbances caused by transverse oscillations of the belt at its fundamental and harmonic frequencies.

Each of these is addressed below.

5.3.1 Internal Friction Losses (Bending Hysteresis)

The evaluation of the hysteresis losses associated with the bending-unbending around the pulleys analyzed a sled configuration with the same driving system dimensions as those of the MIT and JSC units. Internal friction (hysteresis) for metals shows an upper limit which equals 0.2 percent of the total strain energy stored in the configuration. In a drive system, as the belt becomes tangent to the sheave and bends to conform, the stresses change from pure tension to a combined bending and tensile stress with the maximum stress at the outer fibers. When the belt leaves the

sheave, the stresses return to pure tension. The energy loss is therefore the dissipated internal energy connected with just the bending of the belt.

The illustrative comparison example considers a belt 0.127mm thick, 254mm wide operating around a drive drum 0.204mm in diameter with a tension loading of 4000N (same as the MIT-JSC drive systems using cables). In such a configuration, the maximum fiber stress due to the combined tension and bending becomes:

$$S_{max} = \frac{Et}{2\rho} + \frac{T}{wt} \qquad (5\text{-}1)$$

For a steel belt ($E = 2.06 \times 10^{11}$ Pa)

$$S_{max} = 2.52 \times 10^{8} \text{ Pa}$$

Steel belt materials show elastic limits three times the calculated S_{max}; a steel belt would have a conservative operating margin relative to its elastic limits in this application. In considering the bending energy associated with the wraps around the pulleys, the contribution to the total stress from the $Et/2\rho$ term amounts to 1.28×10^{8} Pa.

The elastic energy stored in stressed metal is the sum of all the local stresses (force) times the local strains (distance moved). At any local point the stresses and strains are related by Hookes Law ($S = \varepsilon E$). For the case of bending as in a belt wrapped around a drive pulley, the energy involves an integral expression which is shown derived in figure 5-7. The integral expression takes the form:

$$T = \frac{1}{3} S_{max} \varepsilon_{max} wt \qquad \text{(Fig. 5-7-d)}$$

The value for the strain ε_{max} may be calculated from the bending term for the maximum stress and Hookes Law:

$$\varepsilon = \frac{t}{2\rho} = \frac{0.127(10^{-3})}{2(0.102)} = 0.000622 \text{m/m} \qquad (5\text{-}2)$$

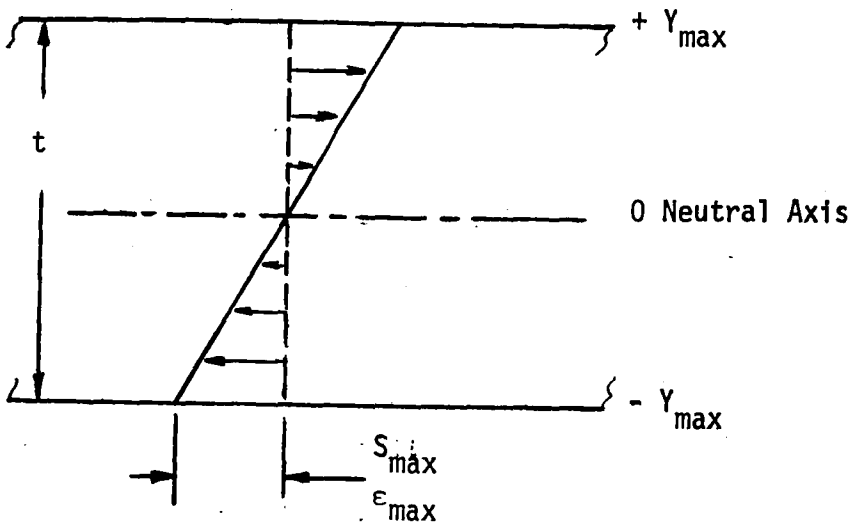

In bending the maximum stress occurs at the inner and the outer fibers.

The force at a distance Y from neutral axis can be expressed as:

$$F_y = w\, S_{max} \frac{Y}{Y_{max}}\, dy \qquad (a)$$

The force acts through a distance equal to the local strain

$$\varepsilon_y = \varepsilon_{max} \frac{Y}{Y_{max}} \qquad (b)$$

The energy stored per unit length of belt is the summation

$$T = 2 \int_0^{Y_{max}} F_y \varepsilon_y\, dy = w\, S_{max} \varepsilon_{max} \int_0^{Y_{max}} \left[\frac{Y}{Y_{max}}\right]^2 dy$$

Thus $$T = \frac{2}{3} S_{max}\, \varepsilon_{max}\, wY_{max}$$

Since $Y_{max} = \frac{t}{2}$

$$T = \frac{1}{3} (S_{max}\, \varepsilon_{max} wt) \qquad (d)$$

Figure 5-7. Bending Energy Stored In A Wrapped Belt

Therefore, substituting in the energy equation (5-7, d) and considering the loss fraction, $0.2(10^{-2})$; the maximum lost energy becomes:

$$\text{Lost Energy} = \frac{2.52(10^{8})(0.000622)(0.254)(0.127)(10^{-3})(0.002)}{3}$$

$$= 0.00337 \frac{Nm}{m} \text{ Max.} \qquad (5\text{-}3)$$

This energy is contained in a half-wrap around each pulley and would equate to a force which generated that much work in a half turn, the equivalent. Friction force would have this magnitude for each pulley in the system. Thus for a two pulley system:

$$F = 2(0.00337N) = 0.0067N$$

If this force were applied to a carriage of a 150Kg total mass, then

$$F = ma, \quad a = \frac{0.0067}{150} = 0.449 \text{ X } 10^{-4} m/sec^2 = 0.449 \text{ X } 10^{-5} g \qquad (5\text{-}4)$$

These levels are more than an order of magnitude below the design limits for thresholds of perception.

5.3.2 Slippage Losses Between the Belt and the Pulley

The geometrical considerations which govern slippage losses and the derivation of the exact expression for predicting such losses are presented in figure 5-8. The expression shows that slippage losses are directly related to the useful (dynamic) stress levels in the belt. From the derivation, the loss ratio is:

$$\text{Loss Ratio} = \frac{Tu}{2AE} \qquad (5\text{-}8,h)$$

If the useful tension force applied by the belt causes an acceleration of 0.5g to a 150kg carriage the tension force is:

$$Tu = ma = 150(0.5)(9.8)$$

$$Tu = 735N$$

Substituting for the case of the steel belt described in 5.1.1 above:

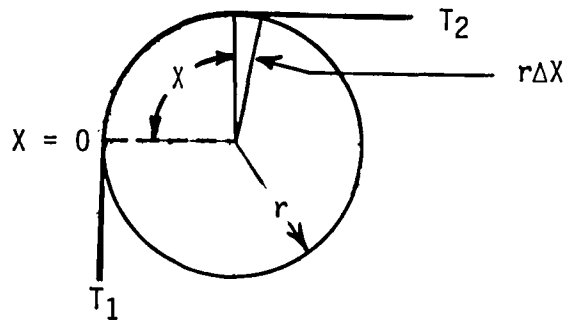

Under no acceleration load the belt tension force is T_1. During acceleration the belt tension force rises to a value T_2 where the belt difference, $T_2 - T_1$ provides the useful work. The wrap angle to the point of no slip at X = 0 is defined by $T_2/T_1 = e^{fX}$. The work lost due to belt elasticity is $(T_2 - T_1)r\Delta X$ where $r\Delta X$ is the stretch in the belt caused by the acceleration loading.

At any X the local useful belt tension force $Tu = (T_2 - T_1)$ is

$$Tu = T_1(e^{fX} - 1) \qquad (a)$$

The strain ε, per unit length

$$\varepsilon = \frac{Tu}{AE} = \frac{T_1}{AE}(e^{fX} - 1) \qquad (b)$$

And the differential strain

$$d\varepsilon = \frac{T_1}{AE}(e^{fX} - 1)rdX \qquad (c)$$

Integrating to X_2 from X = 0 will define the stretch

$$r\Delta X = \frac{T_1 r}{AE}\int_0^{X_2}(e^{fX} - 1)dX = \frac{T_1 r}{AE}\left[\frac{e^{fX}}{f} - X\right]_0^{X_2} \qquad (d)$$

$$= \frac{T_1 r}{AE}\left[\frac{e^{fX_2}}{f} - X_2 - \frac{1}{f} + 0\right] = \frac{T_1 r}{AE}\left[\frac{e^{fX_2} - 1}{f} - X\right]$$

$$r\Delta X = \frac{T_1 r}{AEf}\left[e^{fX_2} - (1 + X_2 f)\right]$$

Figure 5-8. Derivation of Slippage Losses for a Metal Belt

The series expansion for an exponetial:

$$e^{fX_2} = 1 + fX_2 + \frac{(fX_2)^2}{2} + \frac{(fX_2)^3}{6} + \ldots.$$

$$\text{Thus Stretch} = r\Delta X = \frac{rT_1}{AEf}\left[\frac{(fX_2)^2}{2} + \frac{(fX_2)^3}{6} + \ldots\right] \qquad (e)$$

From (a):

$$Tu = T_2 - T_1 = T_1(e^{fX_2} - 1) = T_1\left[fX_2 + \frac{(fX_2)^2}{2} + \frac{(fX_2)^3}{6} + \ldots\right]$$

The stretch may be expressed in terms of Tu by dividing the two series expansions thus;

$$\text{The Stretch} = \frac{rTu}{AEf}\,\frac{\left[\frac{(fX_2)^2}{2} + \frac{(fX_2)^3}{6} + \ldots\right]}{\left[fX_2 + \frac{(fX_2)^2}{2} + \frac{(fX_2)^3}{6} + \ldots\right]} \qquad (f)$$

And using only the first term of the resulting series

$$\text{Stretch} = \frac{rX_2Tu}{2AE} \qquad (g)$$

The useful motion is a rotation equal to rX_2

$$\text{Thus } \frac{\text{Stretch}}{\text{Useful Motion}} = \frac{Tu}{2AE} = \text{loss ratio} \qquad (h)$$

The relative error using only the first term from the series for $fX = 0.2$ is less than 0.5 percent.

Figure 5-8. Concluded, Derivation of Slippage Losses for a Metal Belt

$$\text{Loss Ratio} = \frac{Tu}{2wt} = \frac{735}{2(0.254)(0.000127)(2.06 \times 10^{11})} = 5.51 \times 10^{-5}$$

This ratio would determine the magnitude of the motion reversal transient since it is proportional to the useful (e.g., acceleration) force. In a limit case for an acceleration of 0.5g applied to a 150Kg carriage, the reversal transient becomes:

$$\text{Reversal Transient} = 5.51(10^{-5})(150)(0.5)(9.8)$$

$$\text{Transient} = 0.0396N$$

This force equates to an acceleration transient less than 10^{-4}g which is below any of the measurements for threshold-of-perception.

5.3.3 Transverse Vibrations and Residual Friction Force Considerations

Transverse vibrations of the flat belt cannot be easily analyzed, however, it is believed that the disturbance levels will be orders of magnitude less than the present cable drive because of lower input disturbances and greater air damping. In addition, if it is necessary to add vibration damping devices these can be spaced on the outside of the one-turn belt without interference.

The remaining source of friction considered was that produced by motor brushes. An estimate of these forces indicates that the drive motor should use electronic commutation, and this technique has been developed and is commercially available.

5.3.4 System Considerations for Metal Belt Drives

The utilization of a metal belt drive carries a number of system design implications which must receive consideration. To avoid cueing responses at the times of motion reversal, all the moving elements of the sled must ride on air bearings; for a metal belt drive system the air support requirements are shown in figure 5-9. The particular considerations are summarized below.

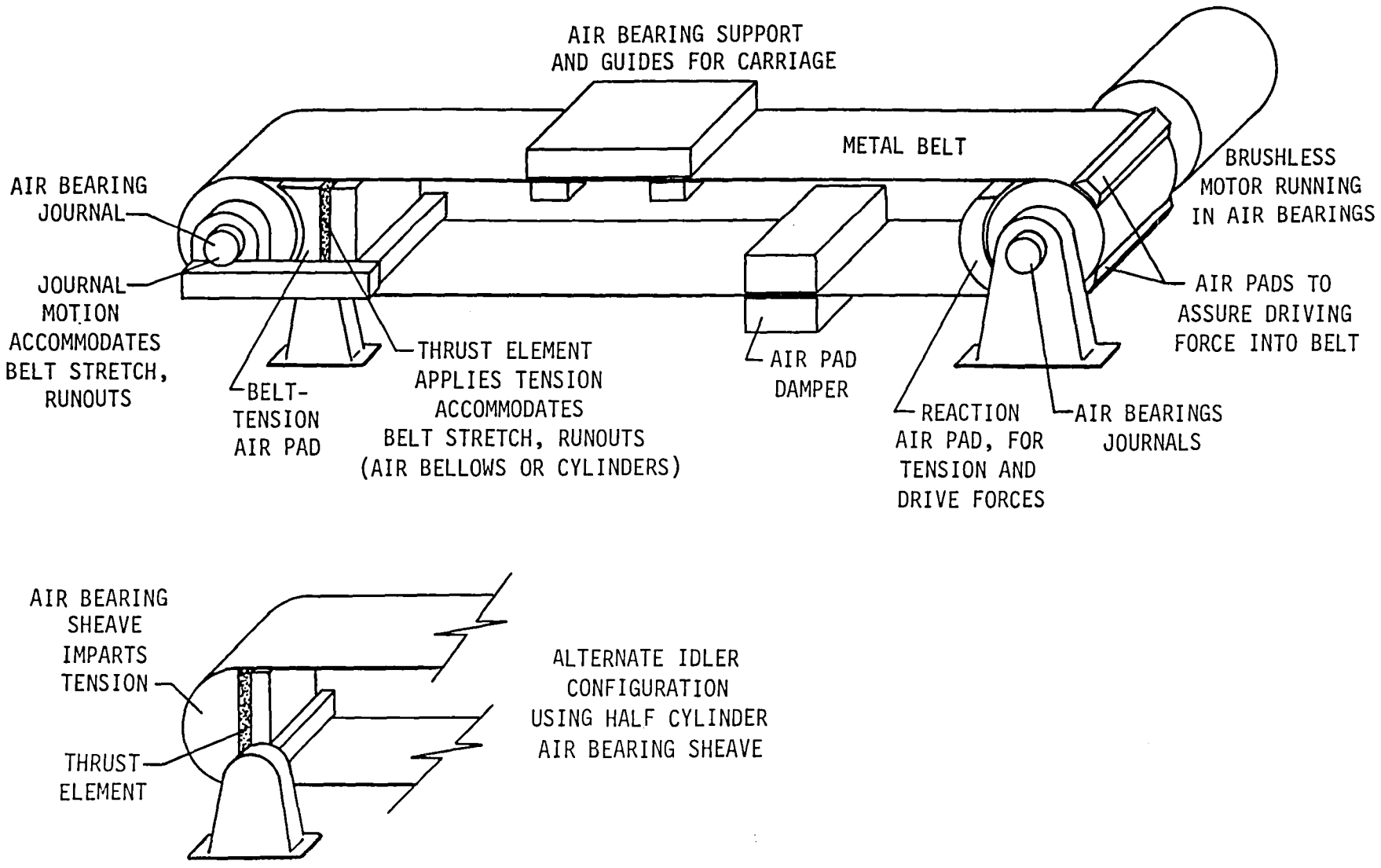

Figure 5-9. System Considerations For a Metal Belt Drive

1. Carriage Support. The requirement for air bearings to support and guide the carriage are described in 5.1 above.
2. Drive Pulley and Motor. These units must rotate in air bearing journals. Some tensile preload will be necessary to prevent a slack belt at extremes of acceleration: Air bearings must accept both the preload and the acceleration forces. Limits on static tension may not permit sufficient driving friction and require an auxiliary air bearing to apply such a load to the belt.
3. Idler Pulley. The idler pulley must apply the preload tension and accommodate any runout or tolerance buildup effects. The preload bearing must be sized to provide the necessary tension while allowing the system sufficient latitude of motion to accommodate manufacturing run-out tolerances in the thickness of the belt and taper in the drums. Metal belt drives must run flat, the conventional technique of crowning the pulleys to generate a centering force on the belt cannot be used; such centering forces imply residual slipping friction effects which will exceed the threshold limits. There will be some side motions of the belt and there will be some motions of the idler pulley relative to the track due to alignment and stretch of the belt; these motions must be accommodated. One potential alternative would be to use a half-circle air bearing as the idler sheave; it could eliminate the need for rotating journals. A second option would introduce lateral freedom in the belt attachment to one end of the carriage (a whiffletree).

In summary, a metal belt drive system offers an approach to a low noise configuration. The system will need to run in air bearings which, thereby, introduce the corresponding complexities. Metal belts and precision drive drums will have a low tolerance for particulate contaminants. A metal belt drive system may need to run enclosed to avoid the effects of particle contamination of the running surfaces.

6.0 SUMMARY AND CONCLUSIONS

The technology evaluations of man-rated acceleration test equipment for vestibular research has provided the data and concepts to support the designs of low noise systems intended for both ground and flight operations. In addition, the study has identified some additional configurations which are compatible with preliminary evaluations or limited scale vertification testing which are discussed in the Appendix. The specific conclusions or findings from this study are as follows:

6.1 Design Limits for Spurious Noises in Sled Systems

A survey of existing published test measurements for thresholds of human perception has permitted the generation of a design limit characteristic. The characteristic is single valued and continuous showing a change with frequency that follows the results obtained from research. The characteristics may be described thus:

a. 0.04 Hz to 3 Hz. Roll off at 1.73 db/octave
   From 0.01g (0.00707 grms) at 0.4 Hz to 0.0003g
   (0.00021 grms) at 3 Hz.

b. 3 Hz to 10 Hz. Level at 0.003g (0.00021 grms).

c. 10 Hz to 100 Hz. Roll up at 1.53 db/octave
   From 0.0003g (0.00021 grms) at 10 Hz to 0.001g
   (0.000707 grms) at 100 Hz.

The establishment of this limit provides a margin below the measured threshold-of-perception values for humans on earth subjected to linear cyclic motion without any visual or other external cues.

6.2 Existing Sleds

Most of the existing horizontal sleds have carriages riding on ball bearings and are driven by tensioned cables with a multiple wrap around the

driving sheave. The configuration generates cueing transients of up to 0.03g (above threshold) coincident with a change in direction of motion. The forces which generate the transients arise from non-linearities in the bearing friction at zero velocity and from friction hysteresis losses in the wrap-unwrap of the cables. There is no obvious way to reduce the transient to a subthreshold level.

A vertical motion sled has been developed which avoids such transients. In this sled, the driving actuator is centered and moved by a continuous-flow hydraulic system such that there are no bearing frictions or sliding contacts in the system.

6.3 Low Noise Sleds Technical Features

The evaluations of technology features produced approaches to the design for low noise sled. The features are:

a. The carriage must be supported and guided by means of air bearings. Commercially developed units have the combinations of load carrying capability and stiffness (motion restraint) to function as support bearings. In addition, measurements have shown that the vibration introduced by the flowing air and the coefficient of friction for the bearings remain below the design limit established for acceleration noise free operation. In addition, evaluations of the air supply pressures and flows show values within the capabilities of small compressors compatible with Shuttle flights. The power requirements for air bearing compressors are also well within the capabilities of the Shuttle.

b. Linear induction motors provide a means for driving the carriage of a sled. Some of the inherent inefficiencies of near-stall motor operations can be reduced by operating the

linear induction motor at the lowest practical frequency. The combination of a linear induction motor drive and air bearings appear to offer the most promising approach to a low noise sled system which could have identical units for both ground and flight testing.

c. Metal belts operating over air supported drive pulleys and drums offer an optional means for propelling a sled. The use of metal belts will add mechanical complexities to the sled system, however, a belt driven system could be built with identical ground and flight units.

APPENDIX

ALTERNATE TESTING TECHNIQUES

CONTENTS

SYMBOLS APPEARING IN THE APPENDIX

C	Linear Force Characteristic for a Spring, N/m
C_s	Linear Force Characteristic for a System of Multiple Springs
E	Linear Extension of a Spring, m
F	Frequency of Oscillation, Hz
g	Acceleration Due to Earth Gravity, 9.8 m/sec^2
I	Mass Moment of Inertia, kg m^4
K	General Force Constant Term, N/m, N/radian
L	Length, m
M	Mass, kg
R	Radius From a Center of Rotation to an Attachment Point, m
r	Radius of Gyration for a Mass Distribution About the Center of Mass, m
T	Tension, N
W	Gravitational Weight, N
Θ	Angular Displacement for a Pendulum, radians
$\ddot{\Theta}$	$d^2\Theta/dt^2$, Angular Acceleration, $radians/sec^2$
κ	Logarithmic Decay Coefficient, 1/seconds
ω	Angular Velocity, radians/sec

APPENDIX

ALTERNATE TESTING TECHNIQUES, INTRODUCTION

In addition to the techniques for obtaining low-noise operations for long-stroke sleds, the study effort identified and evaluated a series of alternate techniques which could provide some portion of the testing capability associated with a sled. Such testing could be utilized to verify the existence of an effect and establish the range or bounds for an environment. The testing would proceed either as a precursor or companion to investigations which needed the long-stroke capabilities. Such alternate techniques appeared as pendulums, as linear motion devices and as an adaptation for industry-used air-bearing tables. Some of the alternates could be configured in a manner which would permit use in a "carry-on" type of experiment for investigations conducted on the mid-deck of the Shuttle.

PENDULUM CONFIGURATIONS

Pendulums present well established straightforward experimental approaches to low-level, low-frequency experimentation. Gravity driven pendulums on earth have provided some of the best measurements available for thresholds-of-perception and can be utilized effectively in almost any configuration which receives the proper attention to detail during the course of design. Pendulums can be applied to a weightless environment; in such cases, the cyclic motion must be mechanically applied, however, the results of the study indicated that useable data can be obtained with a configuration based upon ordinary (i.e., commercially available) wound-wire springs.

Gravity Pendulums Performance Considerations

Gravity driven pendulums provide an effective testing technique for applying sinusoidal oscillating motions over the frequency range 0.20 Hz to

1.0 Hz. The portion of the vestibular response measurement regime compatible with pendulum measurements appears outlined in figure 1. The features and advantages offered by a pendulum can be summarized as follows:

Sinusoidal Motions

Gravity driven pendulums provide sinusoidal motion in the horizontal direction within the limits of the approximate equation of motion

$$\ddot{\Theta} + \frac{g}{L}\Theta = 0 \qquad \text{Solved } \Theta = \Theta_o \cos \omega t \qquad (1)$$

$$\text{where } \omega = \sqrt{\frac{g}{L}}$$

The approximation introduced assumes $\Theta = \sin\Theta$ and at an angular displacement of 0.3 radians (17 degrees), the error is less than 2 percent. For any length of pendulum the horizontal "sinusoidal" component of the motion shows the relationship that the angular deflection in radians is numerically equal to the maximum acceleration expressed in terms of "g" (i.e., an angular deflection of 0.1 radian corresponds to a maximum acceleration of 0.1g). A point on a moving pendulum follows a circular arc, therefore the acceleration vector associated with the movement of a pendulum includes a component parallel to the gravity field which represents the velocity-induced centrifugal force. Consequently, the acceleration vector associated with the motion of a pendulum never sees a zero magnitude. The horizontal component of the acceleration has a maximum at the extremes of angular displacement and changes sign two times for each cycle (i.e., each time the pendulum passes through zero angular deflection). The centrifugal acceleration component has zero values at the extreme angular deflection points and achieves its maximum at the zero deflection point. Thus, the vertical component is always in the same direction, with two maximums per cycle occurring precisely at mid-phase (zero-point) for the horizontal acceleration. The maximum for the vertical component is also directly

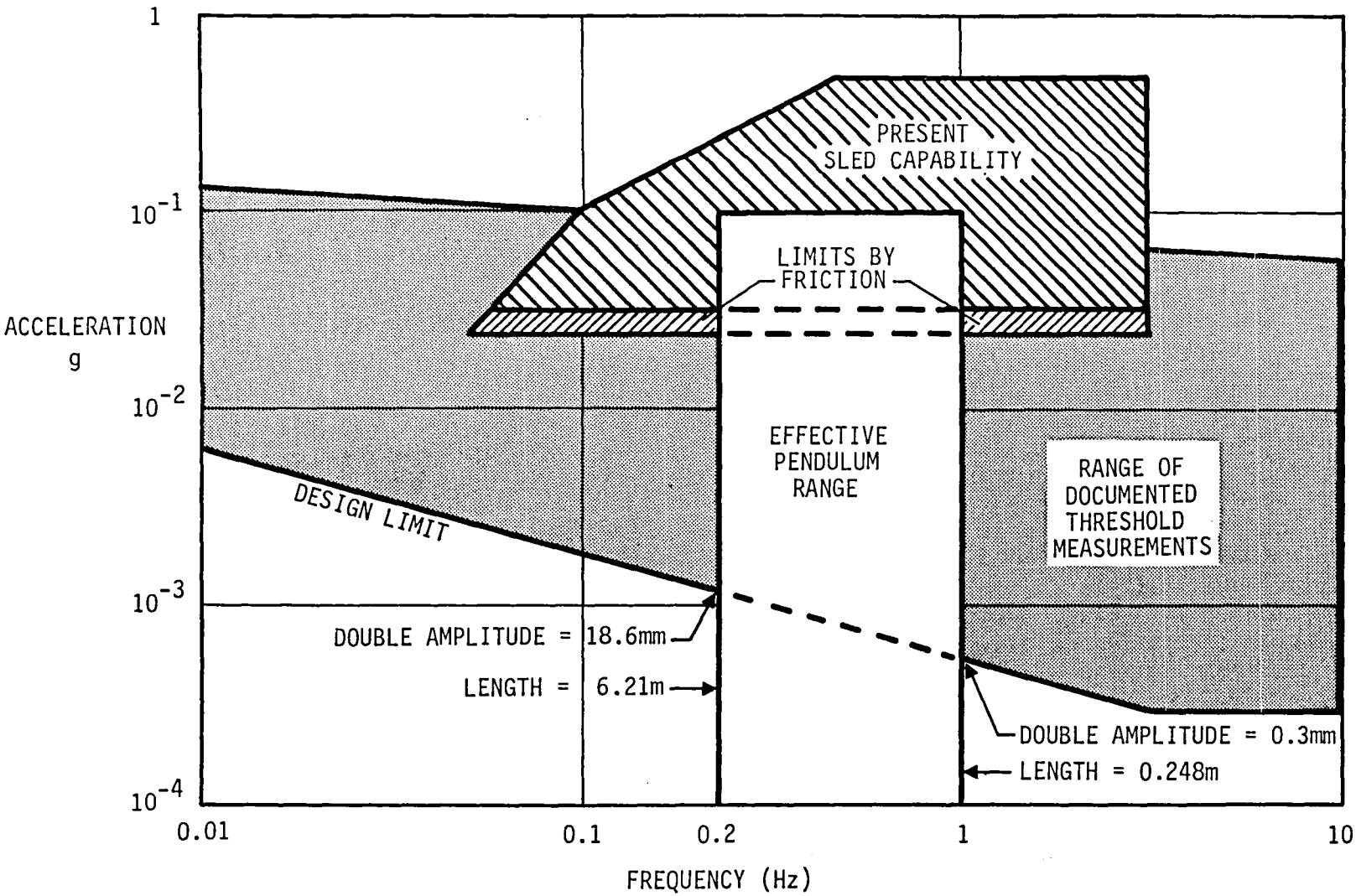

Figure 1. Pendulum Operating Envelope

related to the maximum angular deflection and has a numerical value equal to the square of the maximum deflection also expressed in terms of "g" (i.e., a pendulum with 0.1 radian maximum deflection will have a maximum horizontal component of acceleration of 0.1g, and a maximum vertical component of 0.01g). Thus, the magnitude of the acceleration vector in pendulum motions can be described as a variable with a range in "g" numerically equal to Θ in radians as a maximum and Θ^2 in radians as a minimum. These motion and acceleration considerations appear summarized graphically in figure 2 for the particular case of a 2-meter pendulum.

Pendulum Suspended Test Platforms

If three or more equal-length vertical members form the pendulum support to a horizontal plane, any pendulum motion will keep the plane perpendicular to the gravity field. Any point on the plane or rigidly attached to the plane will move in a circular arc which has a radius equal to the length of the suspension members and a center of rotation directly above that point.

A test subject attached to the plane of such a pendulum experiences no rotational excitations beyond that associated with the movement of the pendulum itself. This feature makes a multiple suspension system (multifilar pendulums) attractive to investigators. Figure 3 shows an example in which an extensive investigation utilized a 4 wire, 4-meter pendulum rig as the excitation source (ref. 4). In the motions of pendulums, the principal parameters of interest relate to the angular deflection, therefore a multifilar pendulum rig is compatible with a variety of linear or angular displacement measuring devices.

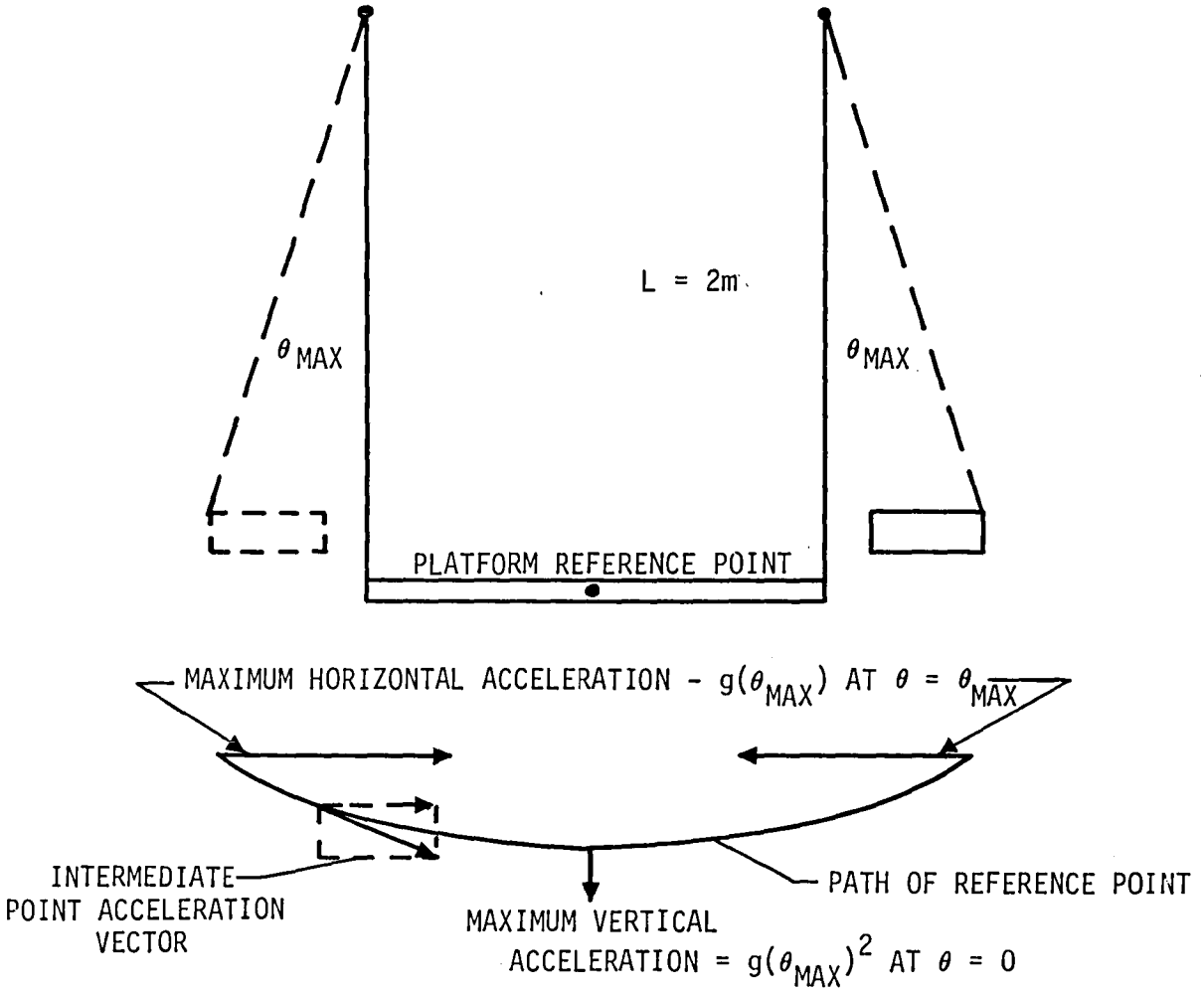

MAXIMUM HORIZONTAL ACCELERATION g	TOTAL HORIZONTAL MOTION	MAXIMUM VERTICAL ACCELERATION g
0.1	40.0 cm	0.01
0.01	4.0 cm	10^{-4}
0.001	4.0 mm	10^{-6}
0.0001	0.4 mm	10^{-8}

Figure 2. Summary of Operating Parameters for a 2 Meter Gravity Driven Pendulum

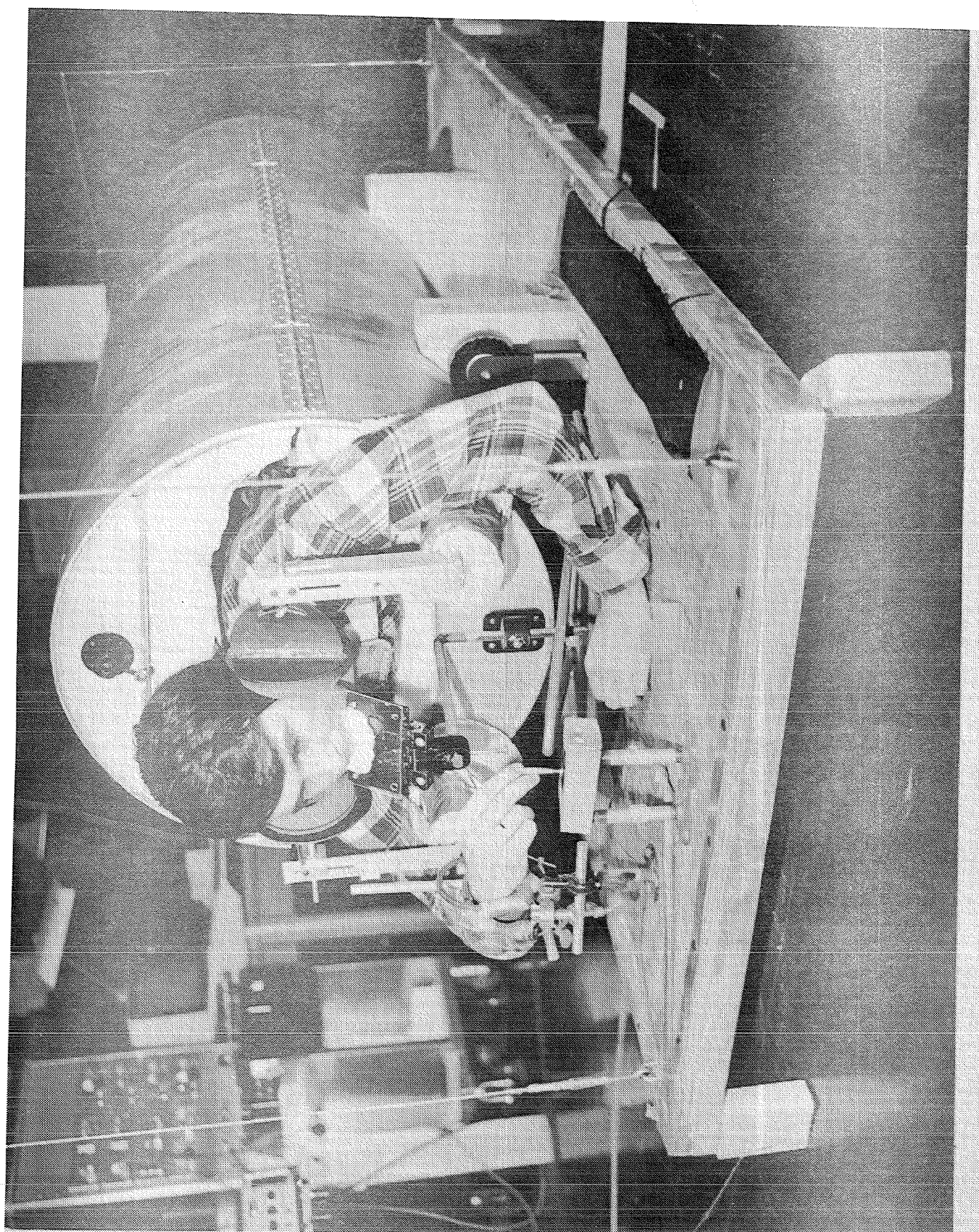

Figure 3. Vestibular Research Pendulum Platform

(Courtesy D. L. Parker, Miami University, Oxford, Ohio)

Frequency Limits

Practicalities define the effective frequency range for gravity driven pendulums. The natural frequency (F) for a pendulum is defined by its length (L) such that

$$F = \frac{1}{2\pi}\sqrt{\frac{g}{L}} \qquad (2)$$

Thus, the upper frequency limit of 1 Hz corresponds to a length of 0.248m which becomes a practical limit for short support members. Measurements in the deflection range 0.001 to 0.1 radian (equivalent accelerations in "g") correspond to double amplitude displacements of 0.50mm to 50mm and require precision measuring equipment. For testing at low frequencies, the length of the pendulum faces practical limits imposed by ceilings in laboratories. For 0.25 Hz the length becomes 3.97m and this dimension approaches the limits imposed by most standard buildings. Access to high bays can extend the operation to lower frequencies; a frequency of 0.2 Hz requires a length of 6.2 meters. The pendulum measurements at 0.1 Hz by Chen (ref. 3) involved a pendulum length of 24.8m (25 meters) and required the equivalent to an eight-story building. (The installation appeared to use an elevator shaft.) For long pendulums, the larger displacements permit the use of less critical instrumentation. At 25m lengths, 0.001g corresponds to a double amplitude displacement of 50mm and 0.1g results in a double amplitude of 5 meters. Building practicalities limit the opportunities for long pendulums in an enclosed (e.g., environmentally controlled) situation, however, the NASA has facilities which would permit enclosed pendulum lengths of up to 150m (KSC and LeRC) and pendulum testing at 0.04 Hz could be proposed; measurements to 0.0001g could be achievable.

Motions and Restraints

A mass hanging from an unrestrained suspension member will experience the same restoring force when moved in any direction, therefore, the frequency of the oscillation is independent of direction. A platform in a multifilar pendulum suspension can be considered free to move in any direction (simultaneous motion along two orthogonal axes with the same frequency and phase but not necessarily to the same amplitude).
In addition, a multifilar pendulum platform has a rotational frequency which also depends upon the length of the suspension members. In the rotational mode the simplified fundamental equation of motion can be shown to take the form

$$I \frac{L}{R} \ddot{\Theta} + RW\Theta = 0 \tag{3}$$

This simplified expression makes the same angular deflection assumptions as the pendulum equation (1) plus the additional simplifying assumption that the arcs in the horizontal plane described by the attachment points can be approximated by a straight line. Since W = Mg, the frequency for oscillations becomes

$$F = \frac{1}{2\pi} \sqrt{\frac{g}{L} \left[\frac{R^2 M}{I}\right]} \tag{4}$$

The moment of inertia may be considered as a circumferentially uniform distribution of the mass at some characteristic radius r (radius of gyration) from the center of mass. Substituting $I = r^2 M$ permits expressing the frequency as:

$$F = \frac{1}{2\pi} \frac{R}{r} \sqrt{\frac{g}{L}} \tag{4a}$$

In practice, the radius of gyration "r" will be less than "R", such that this ratio will be greater than 2 but rarely exceed 3. Real pendulums can have their rotational frequencies very close to their translation frequencies. In

any case, for an unrestrained platform, any misalignment in the application of a driving force will excite both the axes of linear oscillations plus the rotational oscillation. Each of the pendulum experiments cited in the literature has addressed the techniques for application of forces and the means for avoiding or restraining unwanted motions. Skill-of-the-experimenter has been one technique for attaining single mode excitation; positive restraint by means of auxillary wheels controlled the off-axis motions for Chen's 25 meter pendulum system. Redundant diagonal restraints appear as the attainable positive-acting technique for eliminating both the off-axis and rotational modes. For simple pendulums based upon wire rope suspensions, a 4-member main support with redundant diagonals will constrain motion to one direction. The use of diagonals as "Vees" or "X" braces restrains motion by forcing the platform to follow a more sharply curved upward path than the circular arc described by the simple pendulum; response frequencies are increased in all but the direction-of-intent.

Damping of extraneous motions tends to become configuration-specific; however, one potentially useful technique has been experimentally evaluated which provides positive damping to extraneous motions without measurably changing any of the characteristic frequencies. The technique employs a system of diagonal restraints working in conjunction with an elastomerically loaded damper; figure 4 shows the concept. The diagonal ties are brought together at the center of the span and pass between two elastomerically-loaded cylindrical friction surfaces. The combination as illustrated provides a means for uniformly tensioning each section of the diagonal restraint. The system is nearly inactive for motion in the direction intended, however, any torsional excitations or any off-axis lateral deflection will force the diagonals to move relative to the central

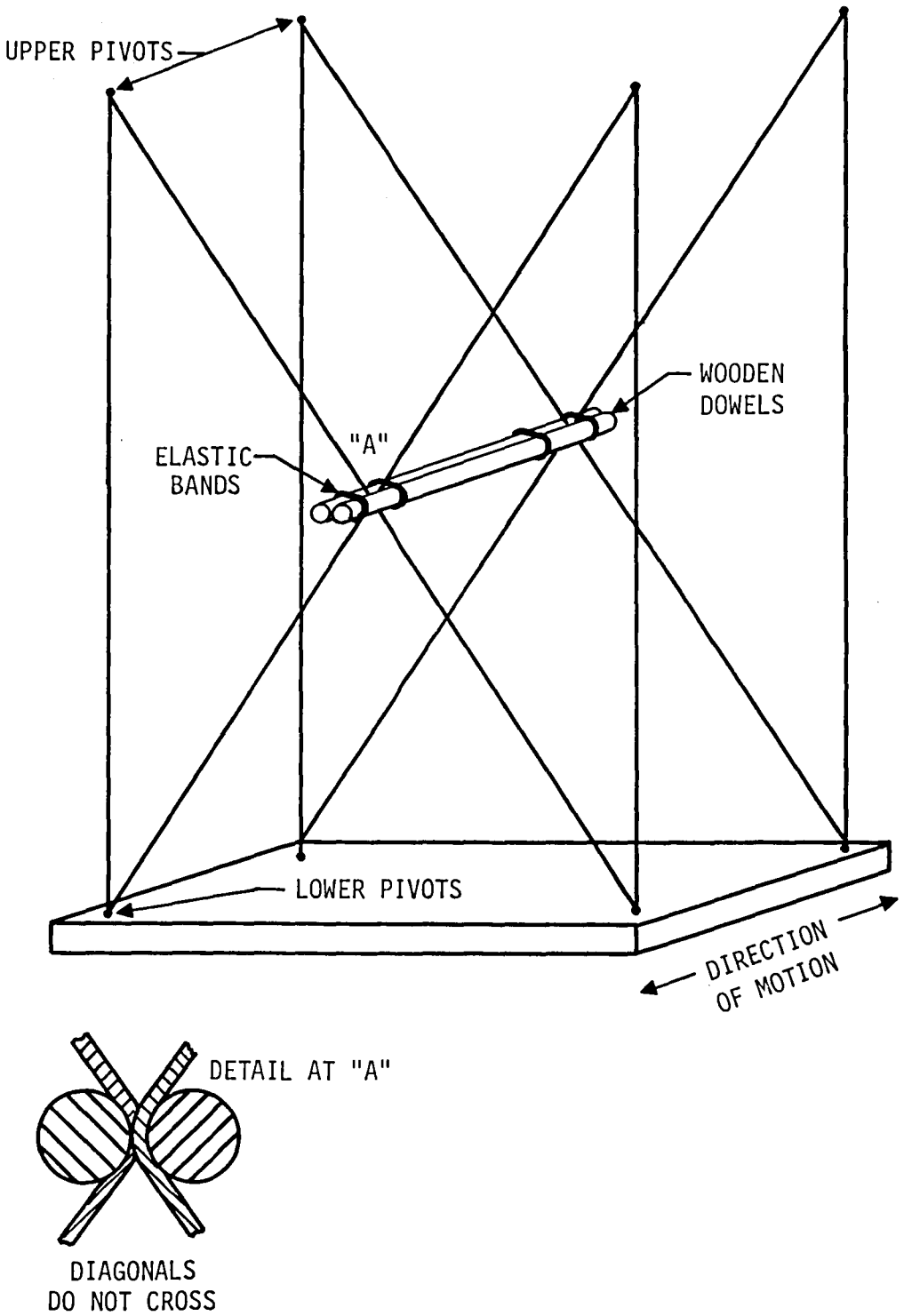

Figure 4. Friction Damper Applied to a Pendulum Platform

restraint and result in a positive damping force. The evaluations performed utilized a 2.1 meter pendulum (frequency 0.38 Hz) with a platform of 30kg that showed an unrestrained torsional frequency of 0.75 Hz. The damping system used wooden dowels (19mm dia.) and eliminated the torsional responses in less than 2 cycles.

Amplitude Decay, Energy Input Requirements

A pendulum test rig deflected and released will follow a course in time which has the form of a damped oscillation:

$$\Theta = \Theta_o e^{-\kappa t} \cos \omega t \qquad (5)$$

The damping term "κ" includes the friction losses in the moving elements plus a contribution due to aerodynamic drag, and none of the contributions may be considered insignificant in testing for threshold-of-perception data. Friction data has been compiled, and the losses associated with pendulums operating in an enclosed volume of air have been addressed by the manufacturers of clocks (ref. 9). These data are helpful, however the "κ" value for a particular rig needs to be determined experimentally. An average decay per cycle:

$$\kappa = 0.002$$

has been observed for one meter pendulums in air, and this value suggests the level of force needed to maintain a constant amplitude. For threshold determinations, the application of forces imposes some particular constraints. In general, the measurements are desired for both the case of increasing amplitude and decreasing amplitude (e.g., sense the onset of motion and also sense the stopping of motion). The decay term provides a means to detect cessation of motion, give it a push and let it coast down.

On the other hand, the increasing function requires care to achieve. For long pendulums where the thresholds will occur at generous amplitudes, hand excitation will provide the needed controls (Chen, ref. 3). Fortunately for the shorter pendulum systems the forces required (0.001g to 0.01g) tend to fall within the ranges and displacements offered by commercially available solenoids. A cyclically driven solenoid exciter is considered an achievable configuration for an experimental operation.

A pendulum test rig will also need a means for releasing the platform without imparting motion. (An auxiliary platform support is generally required while the test subject boards and readies for measurement). The release usually transfers the load into the support wires in preparation for movement. A slow-release hydraulic jack under the platform offers one approach, and such jacks are ordinary items of automotive service equipment.

Auxiliary Force Driven Pendulums

Auxiliary restoring forces can be applied to the oscillating system of a pendulum rig by means of springs or other elastic members. If the restoring force is linear the equation of motion for the oscillating system can be expressed

$$\ddot{\Theta} + \left[\frac{g}{L} + \frac{K}{M}\right]\Theta = 0 \qquad (6)$$

where M is the mass in the oscillating system and K is the force constant in terms of the angle of deflection . The frequency for such a system becomes:

$$F = \frac{1}{2\pi}\sqrt{\frac{g}{L} + \frac{K}{M}} \qquad (7)$$

In the presence of a gravity field, an auxiliary restoring force provides a means to selectively increase the frequency of the system. The auxiliary

forces associated with changing frequencies are related to the geometry of the pendulum system, however, for modest sized systems they are readily obtained. The following examples are offered as illustrations.

Frequency Changes in a Gravity Field

As a basis for showing attainable frequency changes, consider a pendulum system with a length of 3 meters and an oscillating mass of 150 Kg. The natural frequency for such a pendulum is 0.287 Hz. If the frequency is to be raised by a factor of 1.5 to 0.431 Hz, then from equation (7) the contribution from the auxiliary restoring force must be

$$\frac{K}{M} = 4.09, \text{ thus } K = 4.09M \text{ to satisfy } \sqrt{\frac{g}{L} + \frac{K}{M}}$$

If the restoring force is supplied by a spring acting in the path of the pendulum, the spring characteristic becomes:

$$C = \frac{K}{L}, \qquad \text{thus } C = \frac{4.09(150)}{3} = 204.5 \text{ N/m} \tag{8}$$

This value falls close to those measured for the commercial wire-wound units intended for household screen-door closures:

$$C \text{ measured} = 170 \text{ N/m}$$

Pendulums in the Absence of a Gravity Field

Springs can be used to drive a pendulum in the absence of a gravity field. The frequency of the system then becomes a function of the restoring force characteristics and the mass within the oscillating system. For pendulums, practical considerations dictate the application of a force that has a component which will place a tension load on the platform supports. Therefore considerations pertinent to the application of springs will be described in terms of two examples. The configurations to be considered are diagrammed in figure 5. A pendulum length of 2 meters with a platform mass

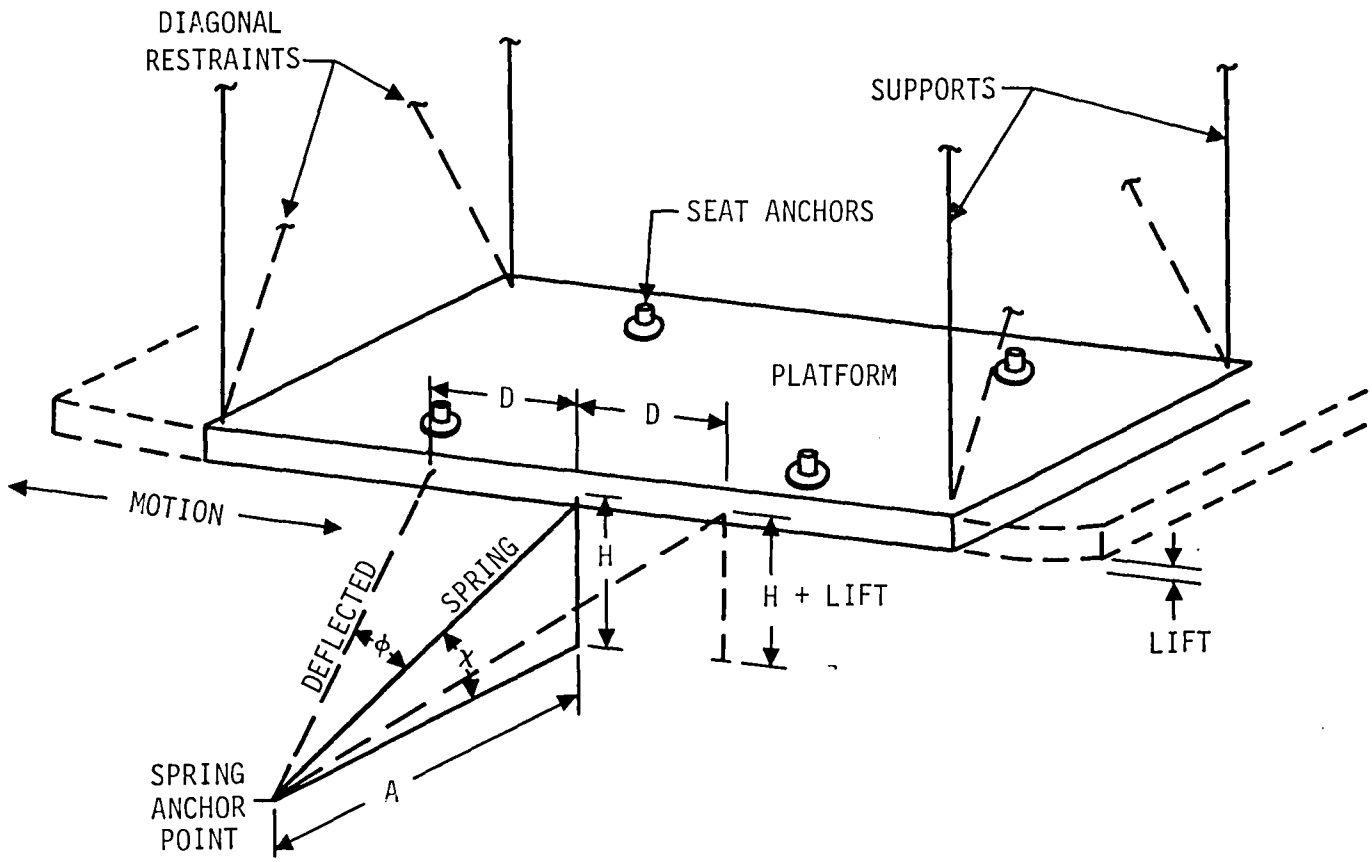

CONFIGURATION 1, PLATFORM WITH TWO SIDE SPRINGS

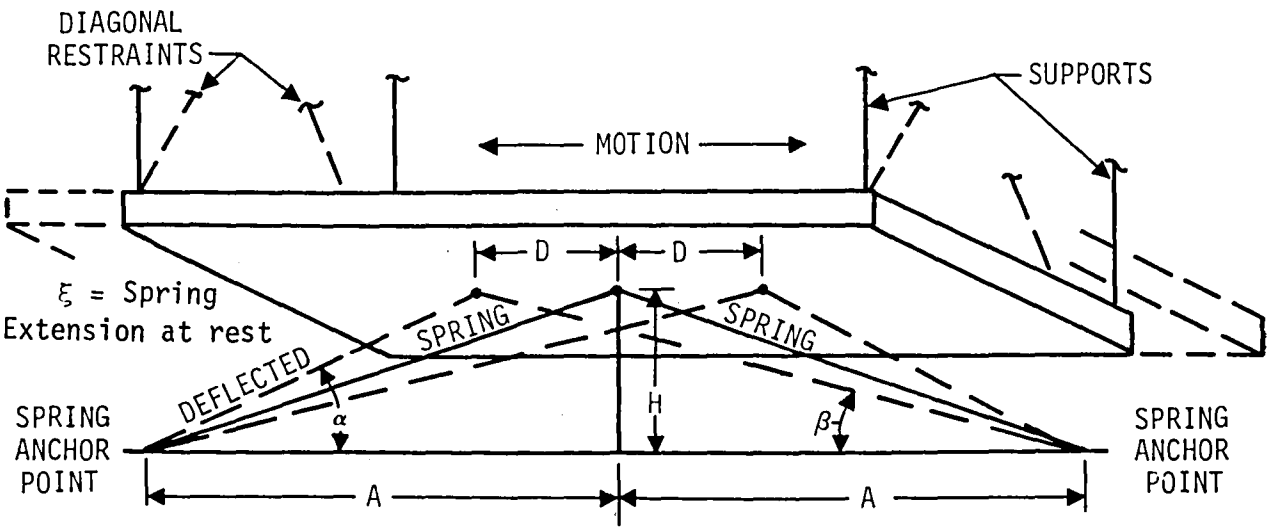

CONFIGURATION 2, PLATFORM WITH DIRECTION-OF-MOTION SPRINGS

Figure 5. Spring Driven Pendulum Concepts

of 150 Kg has been selected such that the entire system is compatible with operation in the mid-deck of the Shuttle. The evaluation will consider a system which would oscillate at the same frequency as a 2-meter gravity driven unit (0.352 Hz). Table 1 summarizes the geometrical considerations pertinent to each of the two configurations.

Configuration 1. Paired Side Springs

A drive system based upon paired side springs would provide a restoring force which would be a linear function of displacement if there were no change-in-length for the spring elements. The cosine-related change-in-length introduces an element of nonlinearity which is parabolic relative to the displacement of the platform. The spring constant for the system is determined by the degree of divergence from linear which can be accepted within the system. For this example, 10 percent has been arbitrarily selected, therefore, at a displacement of 0.2m the contribution to the restoring force from change-in-length must not exceed 14.7N in the direction of motion. Since this is a component of the spring tension, the system force may be expressed as

$$C_s \, \delta \, \text{Sin} \, \Phi = 14.7 \text{ N/m} \quad \text{where Sin} \, \Phi = \frac{0.2}{1.052} \qquad (9)$$

Solving for C_s $= 0.021$m (Change in lengtn for a displacement of 0.2m)

$$C_s = 3682 \text{ N/m}$$

Since the system involves paired springs each side must provide half. For a two spring configuration, the individual spring characteristic becomes 1841N/m. Commercial wound-wire springs are available with these characteristics (i.e., consider ganging 10 screen-door closers). The tension in each spring element with no deflection will be equal to:

$$T = \frac{9 \, \delta \, C}{2} = 347\text{N}$$

TABLE 1. GEOMETRICAL CONSIDERATIONS FOR SPRING DRIVEN PENDULUMS

CONFIGURATION 1. PAIRED SIDE SPRINGS

ASSUMPTIONS		Dimensions, Figure 6-3
Pendulum Length	2m	A = 1 meter
Platform Mass	150kg	D = 0.2m
Frequency	0.352 Hz	H = 0.25m
Restoring Force Constant	735N/m	Lift = 0.01m

GEOMETRICAL LENGTHS	
Spring Element Length No Deflection	1.031m
Spring Element Length Full Deflection	1.052m
Change in Length (δ)	0.021m

SPRING AND LOAD VALUES		
Spring Characteristics	Total 3682N/m	Individual 1841N/m
Spring Extension at "0" Deflection		0.189m (equivalent)
Static Tension in Each Spring Element		347N
Total Load Applied to Supports		168.3N

CONFIGURATION 2. PAIRED AXIAL SPRINGS

ASSUMPTIONS		Dimensions, Figure 6-3
Pendulum Length	2m	A = 1.5m
Platform Mass	150kg	D = 0.2m
Frequency	0.352 Hz	H = 0.25m
Restoring Force Constant	735N/m	Lift = .01m

GEOMETRICAL LENGTHS	
Spring Element Length No Deflection	1.520m
Spring Element Length Maximum	1.718m
Spring Element Length Minimum	1.323m
Change in Length Each Spring	.395m
Change in Length From "0" Deflection Point	.198m

SPRING AND LOAD VALUES	
Spring Characteristics	1880N/m
Spring Extension at "0" Deflection	0.248m
Static Tension in Each Spring Element	466.4N
Total Load Applied to Supports (Both Springs)	153.4N

since the force exerted upon the support wires is defined by the sine of the angle subtended by the height of the platform above the anchor point and including the contribution of the paired system. The force applied to the support members becomes

$$\text{Tension Force} = 168.3\text{N}$$

This example shows an achievable configuration in that wound-wire extension springs are designed to operate with working extensions between 15 and 50 percent of their unloaded length and this case shows a 25 percent extension. The use of commercial screen door closers would require multiple units; however, surveys of commercial supplies show that springs of this type are available and are used in furniture or items of other household equipment. Thus, the system, as described, could be readily configured to replicate the motion of a ground test in a "zero g" environment.

Configuration 2. Paired Axial Springs

A system of paired axial springs offers an alternate. In such a configuration, the difference between the axial components of tension generated by each of the springs becomes the restoring force. If the forces within the springs are not allowed to become zero (some preload at minimum extension), then the force balance becomes (see Configuration 2, Figure 5):

$$C(\xi + \delta)\cos\alpha - C(\xi - \delta)\cos\beta = 735\text{N} \qquad (10)$$

If the system has been configured such that the total motion of the pendulum does not change the cosine terms more than 10 percent from the value for zero deflection, then this nonlinearity may be accepted and the expansion performed in terms of the cosine values for zero deflection. Therefore

$$2C\,\delta = \frac{1.520}{1.5}\,(735\text{N})$$

$$\delta = 0.198\text{m (Change in length from 0 deflection point)}$$

The change in length is that associated with a displacement of 0.2m, thus

$$C = 1880N/m$$

If the springs are designed to operate with a maximum extension equal to 35 percent of the unloaded length, then a maximum extension of 1.718m is 1.35 times the unloaded length, therefore:

$$\text{Unloaded length} = 1.272m$$

This value allows calculation of the tension within each spring element and the loading placed upon the pendulum supports (as shown for case 2, Table 1).

An axial spring system could be achieved using essentially the same springs as for the paired-side configuration if the spring configuration did not involve significant preloading as part of the forming operation. (In general, all wound-wire springs formed with their individual windings in contact, such as screen-door closers, will show some degree of a preload threshold before an extension.)

The nonlinearity of the example shows in the actual difference of forces generated at a deflection of 0.2m.

The Long Spring Component is 829.6N.

The Short Spring Component is 94.2N.

The Difference is 735.4N.

Non-Linear Component 0.4N.

Other Pendulum Concepts

The discussion and examples cited are intended to show the versatility of pendulum test rigs for both ground or spaceflight investigations. Pendulums are not limited to just their gravitationally driven frequencies, and auxiliary drives by springs can be adapted to fit the needs of the experimenter. The examples cited do not exhaust the possibilities for frequency or motion controls; rather they are considered points-of-

departure for an innovative investigator. One option not detailed has been the technique for slowing the frequency of a pendulum in a gravity field. Frequency slowing by mass-tuning has received consideration. Figure 6 shows a concept for a mass-tuned test rig. Mass tuning utilizes the counterbalancing effect of a mass above a pivot to neutralize the gravity-driven restoring force associated with a mass suspended below the pivot and thereby slow the natural frequency of the system. In the concept shown by figure 6, the test subject moves across the top of a circle; a compromise accepted for system stability. Analyses and experiments showed that significant frequency tuning occurs when the moments above the pivot exceed 75 percent of the moments below the pivot. Mass-tuning adds weight to the system, and places severe requirements upon both the pivot bearings and the bending stiffness of the support members. The wrapped-axle concept shown for the pivot bearings and retentions are more fully described in a later section (see Linear Motion by Rolling Friction). For this application the concept allows the use of right circular cylinders as bearings rather than knife edges.

As an additional alternative, the study addressed pendulums supported by metal belts. In such cases the pivots become right circular cylinders joined by endless metal belts (see Figure 7). The concept takes advantage of the very low energy losses in flexing metal belts to achieve smooth motion and the configuration does provide an inherent resistance to off-axis motions. Measurements on such a pendulum showed decay coefficients comparable to those introduced by aerodynamic drag for clock pendulums. The energy loss contribution from the metal belt could not be identified.

REQUENCY LOWERS FROM $F = \frac{1}{2\pi}\sqrt{\frac{g}{L}}$

WHEN WD> 0.75 ML

D~2.5 METERS
L~1.5 METERS

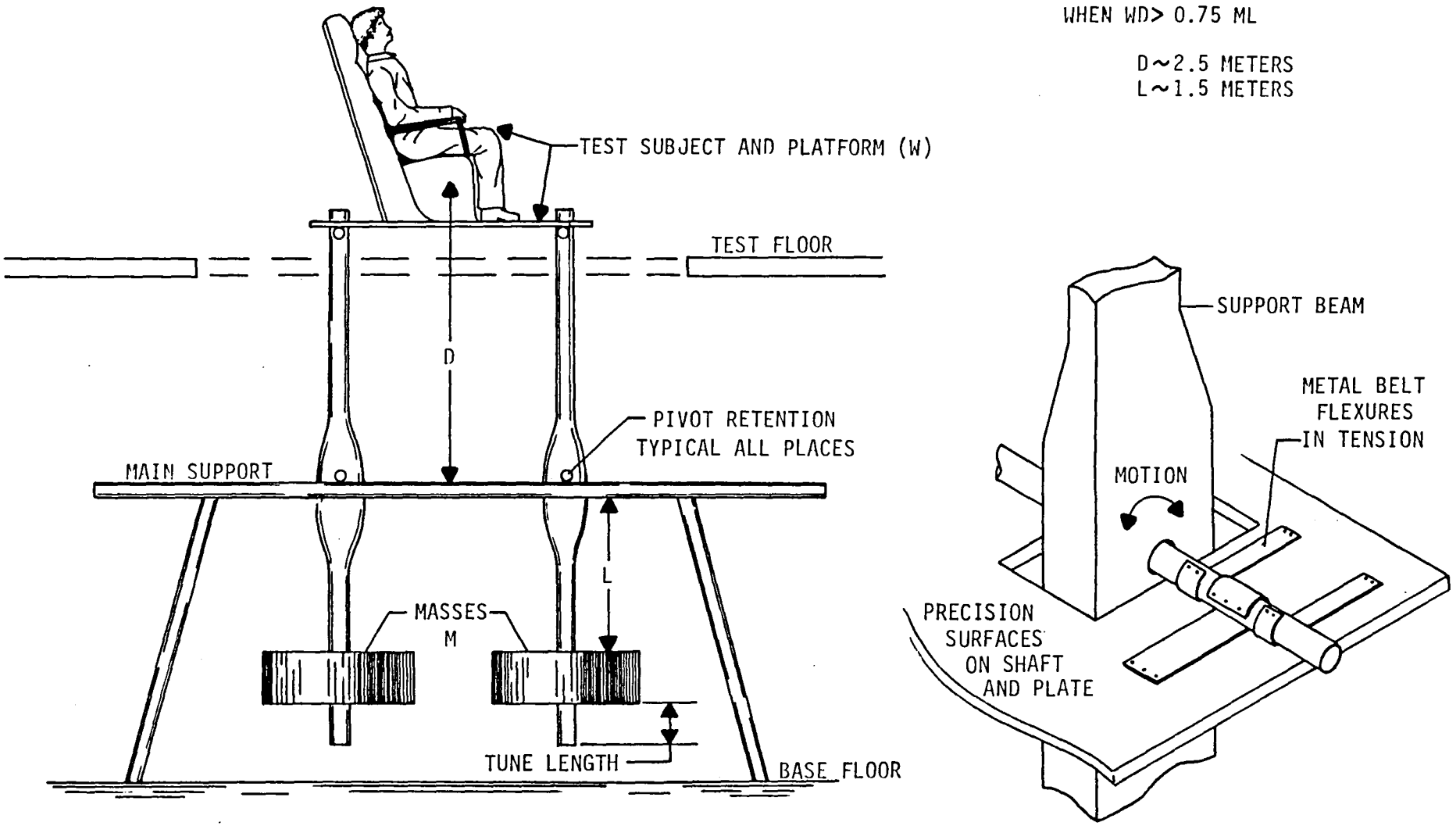

Figure 6. Concept For a Mass Tuned Pendulum Test Rig

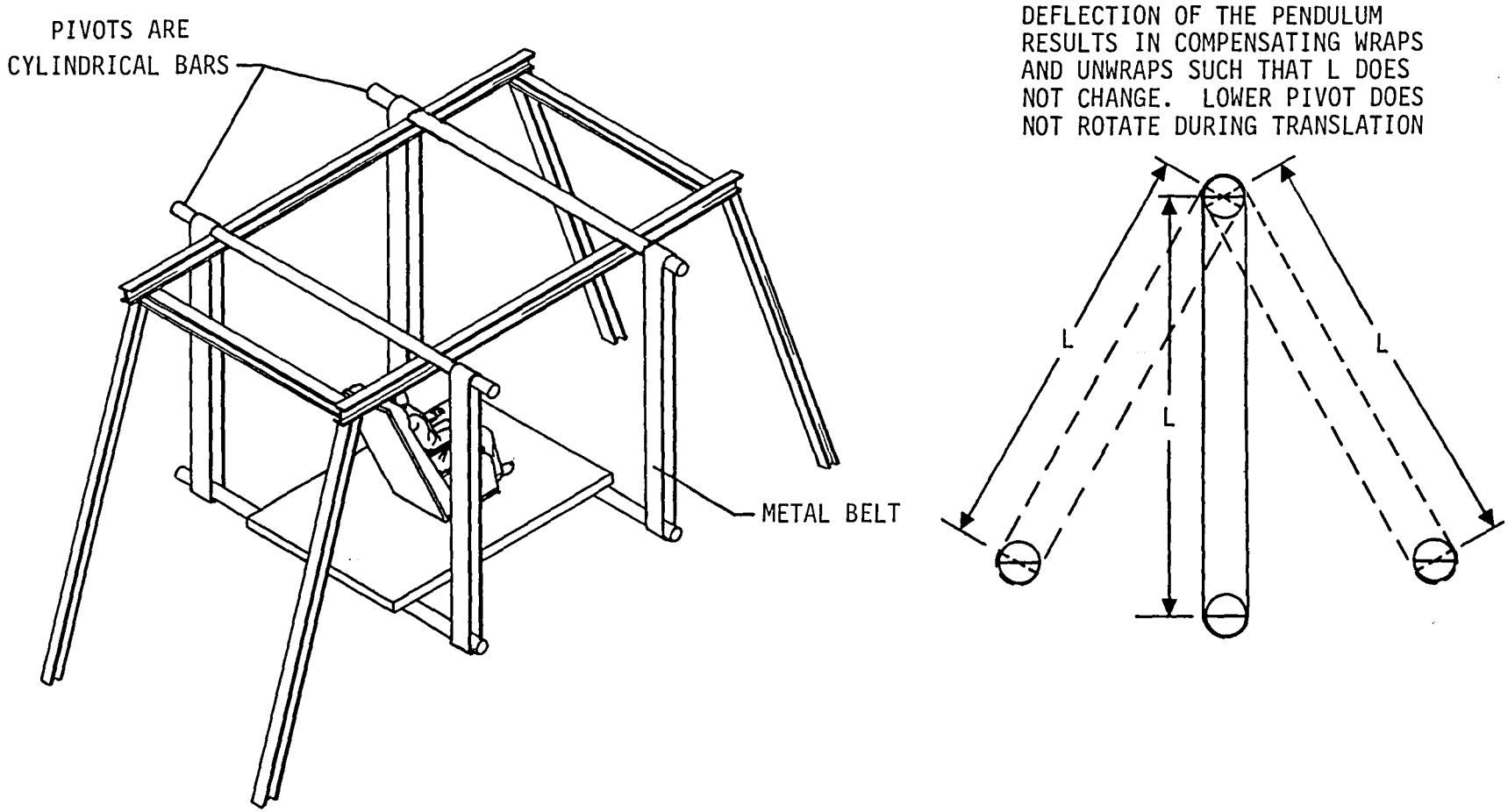

Figure 7. Concept for Pendulum Test Rig Suspended on Metal Belts

LINEAR MOTION DEVICES

The studies of alternate techniques included the evaluation of two concepts which utilized the inherent low noise characteristics associated with metal belt materials or rolling friction.

Flexure Supported Driven Platform

The combination of flexure suspensions and countermoving rotations in supporting arms permits the configuration of a system which will impart a true linear motion; figure 8 shows the concept. In the system, four equal-arm, Vee-shaped pantograph links provide the attachments between the experiment bed and the ground supports. A system of push-rods, tie-rods and an idler-arm provides a linkage interconnection between the pivots on the experiment bed and the pivots at the apex of each pantograph Vee. The combination thus formed is structurally stable.

If the push rods are attached to the idler arm in a manner which moves the experiment bed just two times the distance moved by the pivot point at the Vee in the pantograph arms, then the circular arcs described by the two pantograph arms will cancel such that the platform moves along a straight line. For angular deflections of the idler arm in the range where $\Theta = \sin\Theta$ holds as a valid approximation, the motion is correspondingly linear and straight. Those straight-line conditions are satisfied when the spacing between the attachment points on the idler arm is equal to the length of the individual members of the pantograph arms and the lower push rod attaches to the midpoint of the idler arm. (The ratio of radii is 1:2 along the idler arm). The effective linear stroke for such a system is effectively defined by the length of the individual pantograph arms moving through an angular deflection of 0.3 radians away from the vertical for each member. Thus,

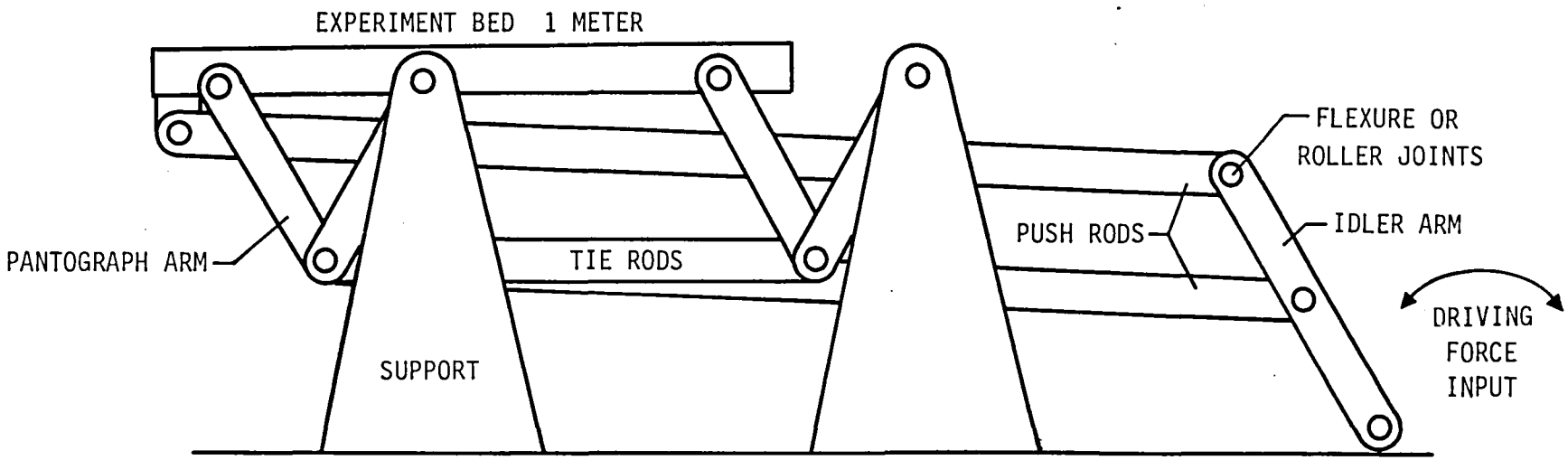

FOR 1 METER STROKE; HEIGHT WOULD BE APPROXIMATELY 1.2m
LENGTH AS SHOWN 1.8m

Figure 8. Flexure Supported Driven Platform

$$\text{Stroke} = 4(\text{arms})(0.3 \text{ rad.})(\text{Arm Length}) \quad (11)$$

$$\text{Stroke} = 1.2 \text{ (Arm Length)}$$

Therefore, a 1 meter stroke implies an arm length of 0.83 meters.

The development of a test rig based upon this concept must address noise-free pivots and the control of alignments within the moving elements. The concept has a potential value for carry-on types of experiments. As an example, a platform with the dimensions of an ordinary chair (seat height of 0.45m) could show a linear travel of 0.24m if configured with linkages of 0.2m length (corresponds to 0.001g at 0.045 Hz from a 120m pendulum). In the design of the experiment the location of the idler arm is not critical; an underseat location can be configured.

The concept can also be modified to produce motions which will follow circular arcs if the positions of the push rods are shifted along the idler arm. In such cases the two pantograph arms do not deflect through exactly the same angles which results in a perpendicular component of motion throughout displacement of the platform. Lowering the attachment point for the lower push rod will reduce the angular deflection at the apex of the Vee, and the platform will travel along an arc with the high point at the center (top of a circle). Lowering the attachment point for the upper push rod will reduce the angle of deflection for the pantograph member attached to the platform, and the motion will take the form of an arc with the low point at the center of motion (bottom of a circle). This feature allows the design of a test rig which can duplicate the motion of long radius pendulums.

Linear Motion with Rolling Friction

A linear motion system can be configured which takes advantage of the low noise associated with rolling friction and metal belt materials. Figure 9 outlines such an approach. The test rig has the appearance of a

MAXIMUM STROKE IS π (WHEEL DIAMATER + AXLE DIAMETER)

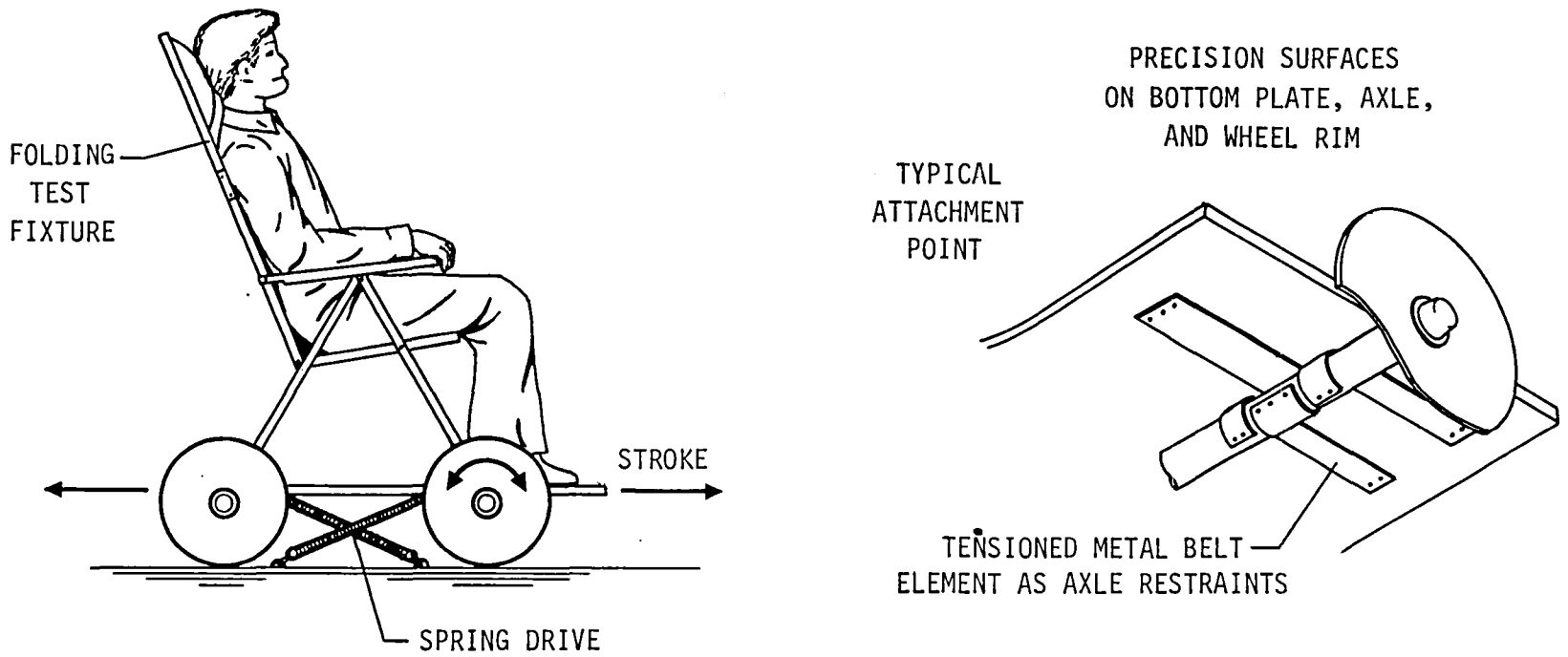

Figure 9. Concept For a Wrapped Axle and Wheel Test Rig Compatible with the Mid-Deck of the Shuttle

four-wheeled cart with solid axles. The concept of half-turn opposed-wraps of metal belt material in tension provides the system stability to keep the platform in proper position relative to the wheels. In oscillation, the platform moves a distance equal to the arc length around the wheel plus the arc length around the axle. The unit does offer straight line motion within a modest sized package. For example, a platform based upon wheels of 0.3m diameter with axles of 50mm diameter could provide a translation of 1.75m. If the distance between the axles was maintained at 0.6m, the envelope dimensions of the rig would remain less than a meter. In practical terms, the achievable stroke will probably be defined by the drive system rather than the rolling limits. A drive system based upon a pair of long springs appears to offer an approach to a maximum stroke configuration. The wrapped axle concept takes advantage of a property inherent in tensioned metal belts. A uniformly tensioned belt at stress levels within the elastic range for the material offers an effective zero resistance to motion through a wrapped type of bending. At the same time the belt provides a stiff resistance against any lateral forces. Therefore if a cylinder has two sets of counter-wrapped belts (e.g., one set at each end), the cylinder will be free to roll but restrained against any axial motion or skewing forces. The rolling motion will occur with just rolling friction losses. For polished hard steel rolling on polished hard steel, the coefficient of rolling friction ranges from 0.0002 to 0.0004 (ref. 10). These values correlate to reversal transients below the threshold design limits.

INDUSTRIAL EQUIPMENT ADAPTATIONS

Some of the precision profile measuring equipment produced for industrial use utilize air bearings to support their moving carriages. These items offer a source for obtaining a relatively long-stroke linear

oscillating test rig for ground usage; figure 10 shows a conceptual application. The industry requirements for precision dictate a straight line linear movement of the carriage with tolerance limits expressed in micrometers. The level of precision is entirely compatible with the type of motion desired for a vestibular test rig. At the present time at least two manufacturers within the U.S. produce equipment with air bearings incorporated in the carriages, and they are available with stroke lengths ranging from 1 meter up to about 5 meters. In general, each item is manufactured in response to an individual order with the unit configured about one of the catalogue-standard sizes and carrying a selection from the catalogue of options which makes a best-fit to the intended use. A unit could be ordered in a configuration intended for oscillatory testing. The cost of such items are in the range associated with machine tools, but are considered modest since they do not have to include the complexities of drives and controls associated with metal cutting systems. The concept illustrated envisions motion in a single axis with oscillations driven by a flat-plate type of spring. The accommodations for the test subject would be bolted to the carriage (accommodations not shown). The driving spring and the driving link are assumed to employ flexure type joints. In addition they would provide the attachments and supports for the air supply lead to the bearings which support the carriage. Table 2 summarizes the performance and pertinent design features for a ground-test rig based upon one of the smaller catalogue size options. In the example the mass assumed for oscillation includes the carriage plus an estimate for a fixture and a human test subject. The data shows an achievable system. The drive spring requirements fall within the capabilities of the carbon steels produced for spring applications.

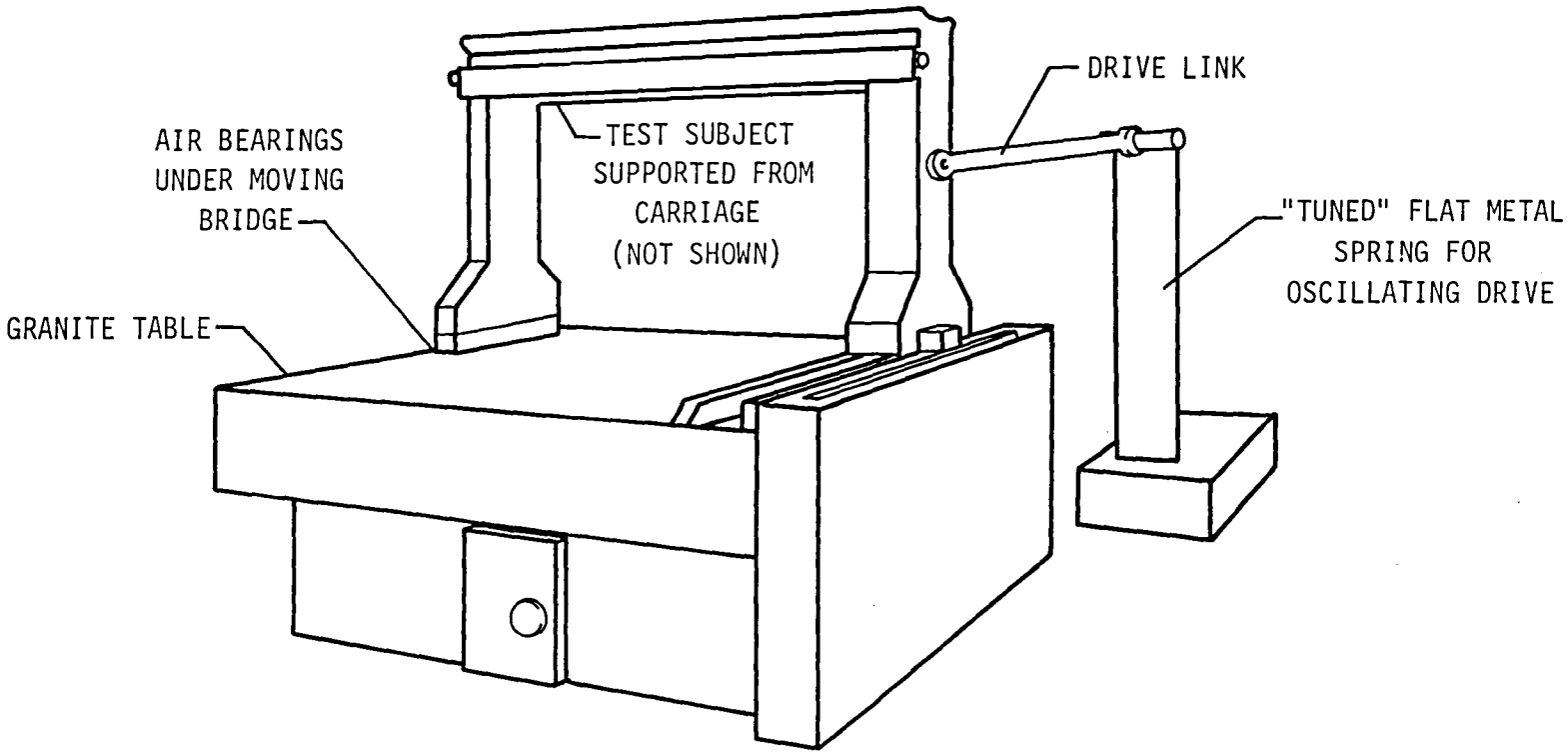

Figure 10. Adaptation of a Commerical Air Bearing Inspection Table to a Linear Motion Test Rig

To summarize, the air bearing carriages utilized in precision profile measuring systems provide a means to obtain a controlled linear motion suitable for vestibular evaluations. A drive system based upon springs appears attainable, and leaves from automotive springs could be evaluated as part of a detail design. The test unit would be suitable for ground use only, the stability and precision required for the table are achieved by heavy bases of either stone (granite) or cast iron. Finally, the physical location for such a unit needs some care in the selection process. These types of equipment have no tolerance for tilt. Their foundations have to be both stiff and stable.

TABLE 2. AIR BEARING TABLE GROUND TEST SYSTEM

PERFORMANCE CAPABILITIES	
Stroke	1 meter
Acceleration Max.	0.1g
Frequency (Equal to Pendulum (L = 5m)	0.222 Hz
SYSTEM DIMENSIONS	
Table Length	2m
Table Width	1m
Carriage Mass	350Kg
Spring Characteristic	686N/m
SPRING DIMENSIONS (FLAT PLATE CANTILEVER SPRING)	
Flexing Length	1.4m
Tip Deflection	0.5m
Deflected Force	343N
Width of Spring	0.213m
Thickness of Spring	6.3mm

Maximum stress is compatible with "Hard Service" for carbon steel spring materials such as SAE 1070 or SAE 1085.

REFERENCES

1. Gundry, A. J. Thresholds of perception for periodic linear motion. Aviat. Space Environ. Med. Vol. 49(5):679-686, May 1978.
2. Bekesy, G. von. The sensitivity of standing and sitting persons subjected to sinusoidal vibration. Akust. Z. 4:360-369. November 1939. (In German)
3. Chen, P.W., and F. Robertson. 1972. Human perception thresholds of horizontal motion. J. Struct. Div. Am. Soc. Civ. Engrs. 98:No. ST8, 1681-1685.
4. Parker, D. E., Gulledge, W. L., Tubbs, R.L. and Littlefield, V.M. A temporary threshold shift for self-motion detection following sustained oscillating linear acceleration. Perception and Psychophysics, Vol. 23, (6), 461-467, 1978.
5. Jaslow, H: Equiperception maneuvers. Aviat. Space Environ. Med. 51(9):867-871, September 1980.
6. A. Soons, Sled Facility Dynamic Performance Test Analysis Report, Doc. No. SLED-R3/127, European Space Agency. Research and Technology Center, Noordwijk, ND, April 1981.
7. Yammamura, S. Theory of Linear Induction Motors, Second Edition, Holsted Press, John Wiley and Sons Inc. 1979.
8. Laithwaite, E. R., Nick, G. F., Linear induction motors for low-speed and standstill application. Proc. IEE, Vol. 113, No. 6, June 1966.
9. Rawlings, A. L. The Science of Clocks and Watches. Pittman Publishing Co., 1944.
10. Marks, L. S., Baumeister, T. Mechanical Engineers Handbook, 6th Edition:3-45, McGraw-Hill Book Co., 1958.

1. Report No.	2. Government Accession No.	3. Recipient's Catalog No.
NASA CR-172160		

4. Title and Subtitle	5. Report Date
Technology Evaluation of Man-Rated Acceleration Test Equipment for Vestibular Research	September 1983
	6. Performing Organization Code

7. Author(s)	8. Performing Organization Report No.
I. Taback, R. L. Kenimer, A. J. Butterfield	
	10. Work Unit No.

9. Performing Organization Name and Address	11. Contract or Grant No.
The Bionetics Corporation 20 Research Drive Hampton, VA 23666	NAS1-16978
	13. Type of Report and Period Covered
12. Sponsoring Agency Name and Address	Contractor Report
National Aeronautics and Space Administration Washington, DC 20546	14. Sponsoring Agency Code

15. Supplementary Notes

Langley Research Center Technical Monitor
George L. Maddrea, Jr.
Final Report

16. Abstract

This study addresses the considerations for eliminating acceleration noise cues in horizontal, linear, cyclic-motion sleds intended for both ground and shuttle-flight applications. The principal concerns are the acceleration transients associated with change in direction-of-motion for the carriage. The study presents a design limit for acceleration cues or transients based upon published measurements for thresholds of human perception to linear cyclic motion. The sources and levels for motion transients are presented based upon measurements obtained from existing sled systems. The approaches to a noise-free system recommends the use of air bearings for the carriage support and moving-coil linear induction motors operating at low frequency as the drive system. Metal belts running on air bearing pulleys provides an alternate approach to the driving system. The appendix presents a discussion of alternate testing techniques intended to provide preliminary type data by means of pendulums, linear motion devices and commercial air bearing tables.

17. Key Words (Suggested by Author(s))	18. Distribution Statement
Vestibular Testing Thresholds-of-Perception Acceleration Sleds	Subject Categories 51 and 54 Unclassified - Unlimited

19. Security Classif. (of this report)	20. Security Classif. (of this page)	21. No. of Pages	22. Price
Unclassified	Unclassified	99	A05

For sale by the National Technical Information Service, Springfield, Virginia 22161

End of Document